Study on Functions of Histone Variant H2A.Z for the Maintenance of Heterochromatin Integrity

ヘテロクロマチンにおけるヒストンバリアント

H2A.Z の機能に関する研究

Laboratory of Bioorganic Chemistry,
Graduate School of Chemical Sciences and Engineering,
Hokkaido University

Kazuki Tsukii

2022

Table of Contents

Abstract

Heterochromatin, a silent chromatin is involved in many biological processes, such as gene silencing, development, chromosome segregation, and genome integrity. Post translational modifications of histone tails are crucial for heterochromatin formation. Methylation of histone H3 at Ly9 (H3K9me) is a well conserved heterochromatic modification. For the formation and maintenance of heterochromatin, RNAi-dependent and -independent pathways redundantly functions and recruits H3K9 methyltransferase Clr4 to heterochromatic region. HP1 recognizes H3K9me and forms highly condensed chromatin structure. HP1 recruits not only silencing factors but also anti-silencing factor Epe1, a H3K9me demethylase, to heterochromatic regions, suggesting that the competition between silencing factors and anti-silencing factors is important for proper maintenance of heterochromatin. As well as histone modifications, histone variants also play important roles. Especially, H2A.Z is one of the most evolutionally conserved histone H2A variant. H2A.Z has been implicated in many biological processes, including gene regulation, mammalian development, DNA replication, and stress response. In particular, the function of H2A.Z in euchromatic gene regulation is well studied. H2A.Z is highly enriched at gene promoter and is required for the proper transcription. However, its function and deposition mechanism in heterochromatin is still unclear. Here, I show that H2A.Z plays multiple roles in fission yeast heterochromatin. In fission yeast, H2A.Z is loaded into nucleosomes at TSS of euchromatic gene by the H2A.Z loader, SWR complex. While a small amount of H2A.Z localizes at pericentromeric heterochromatin compared to euchromatic gene promoter, loss of H3K9me induces the accumulation of H2A.Z, which is dependent on the SWR complex. The accumulated H2A.Z suppresses heterochromatic non-coding RNA transcription. This transcriptional repression activity requires the N-terminal tail of H2A.Z, which is involved in the regulation of euchromatic gene transcription. Additionally, RNAi defective cells, in which a substantial amount of H3K9me is retained by RNAi-independent heterochromatin assembly, also accumulate H2A.Z at pericentromeric heterochromatin. The additional loss of H2A.Z in these cells abolishes H3K9me. Moreover, loss of H2A.Z in RNAi defective cells decreased H3K9me at the *mat* locus heterochromatin and subtelomere heterochromatin, where RNAi is dispensable. However, H2A.Z is not required for the maintenance of artificially formed ectopic heterochromatin which is

maintained by RNAi-independent mechanism in the absence of Epe1, suggesting the indirect effects of H2A.Z for RNAi-independent heterochromatin assembly. As Epe1, an eraser of H3K9me is responsible for the decrease of H3K9me in RNAi mutants, loss of Epe1 restored the H3K9me in RNAi and H2A.Z double deletion mutants. These results suggest that H2A.Z facilitates RNAi-independent heterochromatin assembly by antagonizing the demethylation activity of Epe1. Furthermore, loss of H2A.Z caused silencing defects at subtelomeric heterochromatin without affecting H3K9me. Since Epe1 also has a transcription activation domain at N-terminus, overexpression of Epe1 results in transcriptional activation at pericentromere without affecting H3K9me. Loss of H2A.Z in Epe1-overexpressig cells synergistically increases the transcription, and the subtelomeric silencing defect in H2A.Z deletion mutant is suppressed by loss of Epe1. These results suggests that H2A.Z suppresses Epe1-mediated transcriptional activation, which is required for subtelomeric gene repression. Taken together, this study provides novel evidence that H2A.Z plays diverse roles in chromatin silencing.

1. Introduction

1-1 Epigenetics

In eukaryotic cells, the structure of chromatin, which is composed of DNA and histone octamers (Figure 1), is dynamically regulated and plays important roles in many cellular processes, such as the control of gene expression, DNA replication, chromosome segregation, and development (Allshire and Madhani, 2018; Grewal and Jia, 2007). Histone modification is a key factor in the regulation of chromatin; specific histone modifications create recognition sites for "reader" proteins that regulate chromatin structure and function.

There are two types of chromatin structures: euchromatin and heterochromatin. Euchromatin is a transcriptionally active chromatin. In euchromatin, H3 and H4 are highly acetylated, and these histone acetylations recruit transcription factors which contain acetylated lysine biding domain, bromo domain, resulting in active transcription (Clayton et al., 2006; Zeng and Zhou, 2002). On the other hand, heterochromatin is a silent chromatin. The methylation at Lys9 of H3 (H3K9me) is a well conserved heterochromatic modification in fission yeast and mammals (Allshire and Madhani, 2018; Grewal and Jia, 2007). Heterochromatin Protein 1 (HP1) binds to H3K9me through its chromodomain and forms highly condensed structure via homodimerization, which sequesters heterochromatic domains in the nucleus (Allshire and Madhani, 2018; Grewal and Jia, 2007; Larson et al., 2017). HP1 recruits various silencing factors such as histone deacetylases, resulting in the formation of silent chromatin (Fischer et al., 2009). In higher eukaryotes, DNA methylation and H3K27me are also found in heterochromatic region and form transcriptionally silenced chromatin (Rose and Klose, 2014; Wiles and Selker, 2017). These modifications are dynamically regulated during cell cycle and important for gene silencing, chromosome segregation, and maintenance of genome integrity (Allshire and Madhani, 2018; Grewal and Jia, 2007).

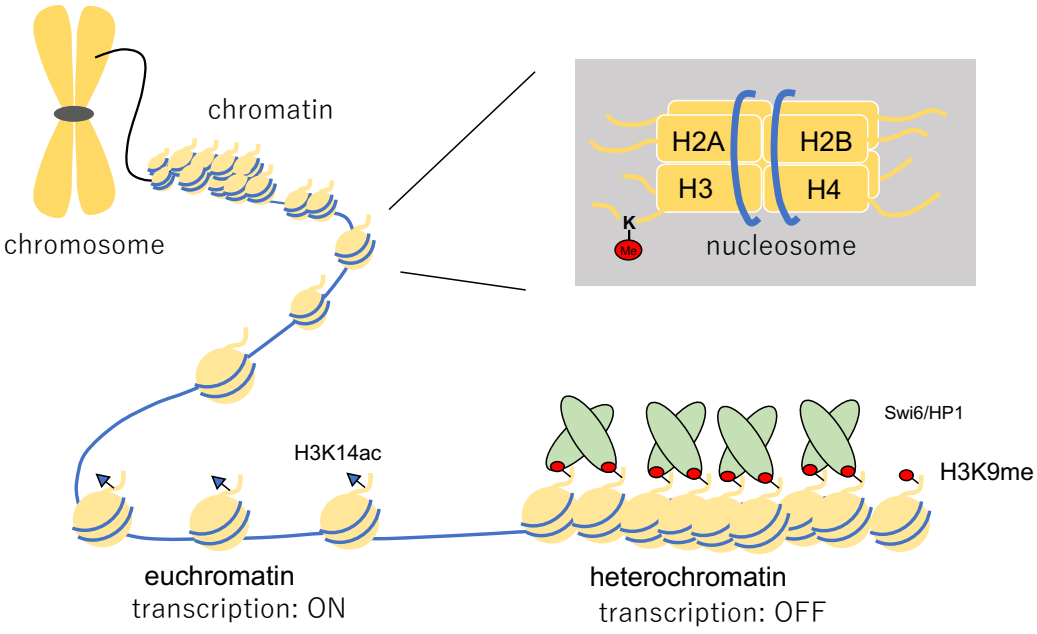

Figure 1 chromatin structure

DNA wraps around histone octamer, two copies of H2A, H2B, H3 and H4, which forms chromatin structure. The modifications at histone tails are important for the regulation of chromatin structure. In euchromatin, histone acetylation (for example, acetylation at H3K14) are highly occupied, resulting in gene activation. By contrast, in heterochromatin, H3Lys9 is methylated. HP1/Swi6 recognizes H3K9me and forms highly condensed chromatin structure via homodimerization. HP1 also recruits silencing factors, resulting in the establishment of transcriptionally silent state.

1-2 Maintenance of heterochromatin

The fission yeast *Schizosaccharomyces pombe* is an excellent model organism to study the diverse nature of heterochromatin, as it possesses a fundamental and well conserved chromatin regulation system. Fission yeast heterochromatin is determined by H3K9me, noting that there is no DNA methylation and H3K27me. While mammals contain several proteins which redundantly works in heterochromatin formation, in fission yeast, heterochromatin is mostly regulated by sole protein which enables us to elucidate fundamental heterochromatic regulation systems.

In fission yeast, there are three constitutive heterochromatin domains: the pericentromere, the mating type region (*mat* locus), and the subtelomere region (Figure 2A). Each of these regions contain *dg/dh* repetitive elements (Figure 2B) (Grewal and Jia, 2007). RNAi contributes to heterochromatin maintenance and the establishment in these loci (Figure 3A) (Hall et al., 2002; Jia et al., 2004; Kanoh et al., 2005). *dg/dh* ncRNAs are transcribed by RNA polymerase II (Kato et al., 2005), and RNA dependent RNA polymerase complex (RDRC) synthesize double strand RNA (Motamedi et al., 2004). These dsRNAs are processed into small interference RNA (siRNA) by Dcr1 (Provost et al., 2002). Then siRNAs are loaded into Ago1, a component of RNA induced transcriptional silencing (RITS) complex, which targets nascent RNA using siRNA as a guiding molecule (Verdel et al., 2004). RITS recruits H3K9me "writer" CLRC complex, which contains Clr4, a homolog of fruit fly H3K9 specific histone methyltransferase Suv3-9, which enables spreading of H3K9me (Bayne et al., 2010). Then, fission yeast HP1 homologues Swi6 and Chp2 recognize H3K9me and induce heterochromatin formation.

Even in RNAi-deficient cells, H3K9me is retained at an intermediate level in the pericentromeric region through the function of a second heterochromatin formation system, which contains many factors including RNA processing machinery (Buscaino et al., 2013; Chalamcharla et al., 2015; Reyes-Turcu et al., 2011; Shipkovenska et al., 2020; Tucker et al., 2016). Moreover, H3K9me levels are maintained without RNAi at the *mat* locus and in subtelomeric heterochromatin. DNA-binding protein Atf1/Pcr1 recruit Clr4 to the *mat* locus (Jia et al., 2004). In subteromeric heterochromatin, Taz1, a component of telomer protection complex Shelterin binds telomeric repeat element, and Ccq1, a component of Shelterin

recruits Clr4 to the telomeric heterochromatin (Kanoh et al., 2005; Wang et al., 2016; Zofall et al., 2016). In addition to these Clr4 recruitment mechanisms, Clr4 self-propagation can enable faithful H3K9me inheritance; Clr4 can bind to H3K9me via the chromodomain and deposit H3K9me onto neighboring nucleosomes (Figure 3B) (Audergon et al., 2015; Nakayama et al., 2001; Ragunathan et al., 2015).

Epe1, an "eraser" of H3K9me, is recruited to heterochromatin by Swi6 through direct interaction (Zofall and Grewal, 2006), preventing the spreading of heterochromatic domains over heterochromatin-euchromatin boundaries (Ayoub et al., 2003). Furthermore, Epe1 has a transcription activation domain at N-terminus (Sorida et al., 2019). Thus, overexpression of Epe1 increases transcription at heterochromatic region, resulting in high histone turnover rate (Aygun et al., 2013; Trewick et al., 2007). Epe1 prevents ectopic heterochromatin formation via its N-terminus transcription activation domain (Sorida et al., 2019). These findings indicate that the balance between "writer" and "eraser" is important for H3K9me maintenance.

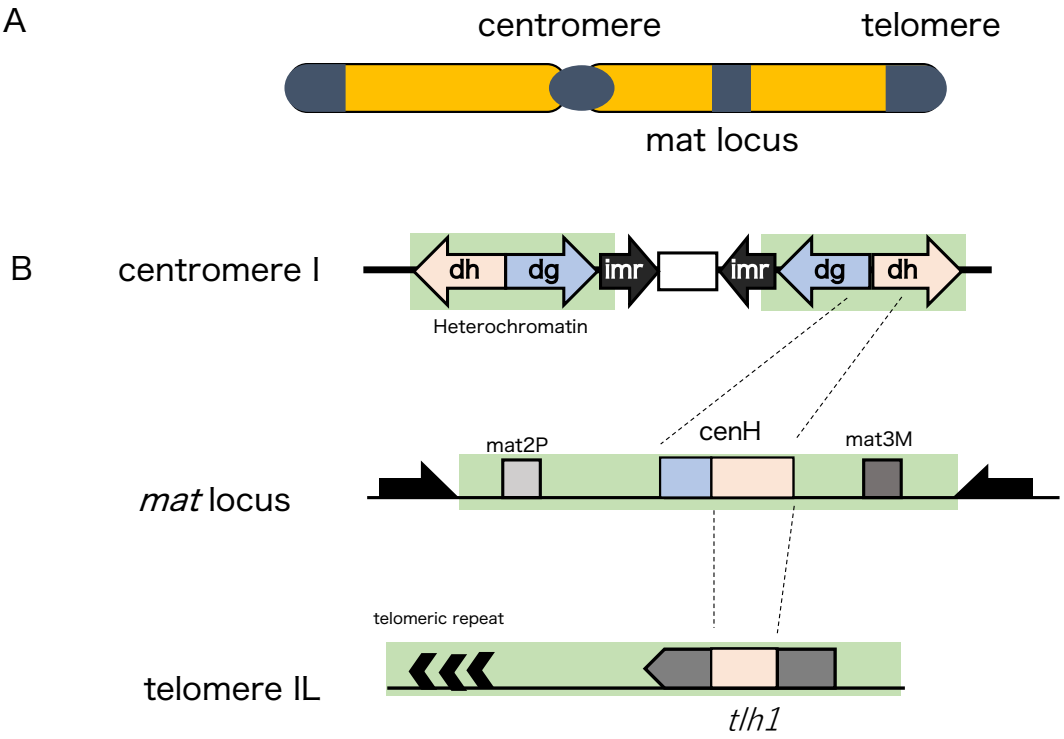

Figure 2 S. pombe heterochromatin

A) S. pombe has three chromosomes. Heterochromatin is formed at centromeres, telomeres, and mating type locus (*mat* locus; at chromosome2).

B) Each heterochromatic region (green box) contains *dg*/*dh* sequence. Center region of centromere is surrounded by inverted repeats which contain *dg*, *dh*, and *imr* element. *mat* locus is located at chromosome 2 and contains *dg/dh* homologous element which is celled *cenH* element. Subtelomeric genes, *tlh1*, which encodes telomere-linked DNA helicase contains centromere homologous repeats, where RNAi occurs.

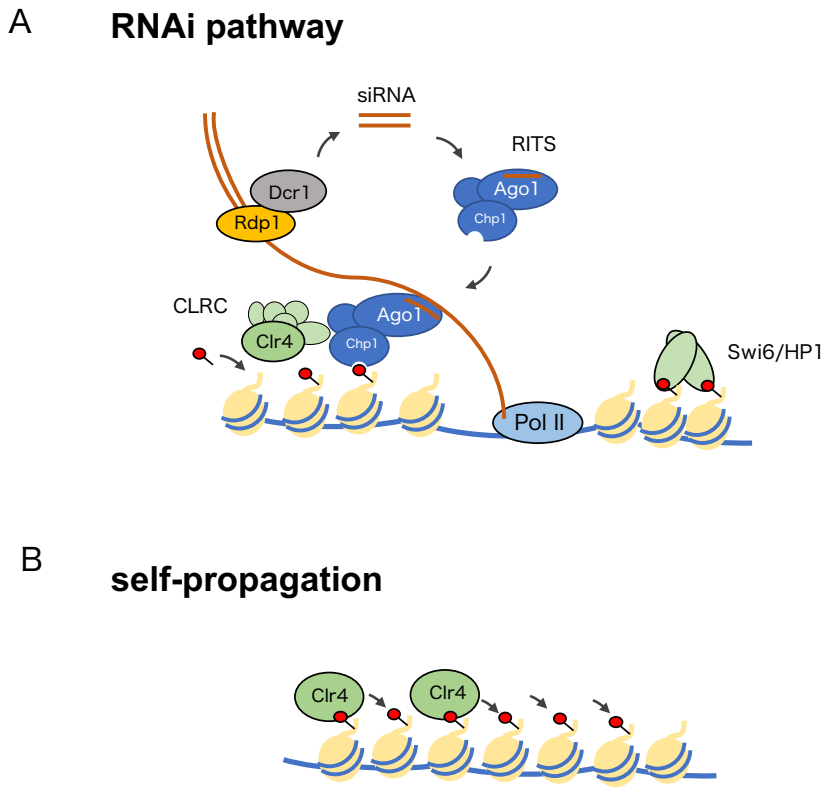

Figure 3 mechanisms of heterochromatin assembly

A) RNA polymerase II transcribes heterochromatic non-coding RNA. Rdp1 synthesizes double strand RNA (dsRNA) and Dcr1 processes into small interfering RNA (siRNA). Ago1, a component of RITS binds siRNA, which targets to complementary nascent RNA. Chp1, a component of RITS binds H3K9me and partly contributes RITS recruitment. Then, RITS recruits CLRC complex which contains Clr4, H3K9 methyltransferase, resulting in the deposition of H3K9me.

B) Clr4 not only has H3K9 methyltransferase domain, SET domain, but also H3K9me-binding domain, chromodomain. Thus, Clr4 itself can spread H3K9me.

1-3 Histone variant H2A.Z for gene regulation

Histone variants, in addition to post-translational histone modifications, play important roles in chromatin regulation. The histone H2A variant H2A.Z is one of the most evolutionally conserved histone variants. H2A.Z has several unique amino acids compared to canonical H2A (Figure 4). Especially, acetylations at N-terminus lysine and extended acidic residues in docking domain are well conserved features of H2A.Z (Giaimo et al., 2019; Zlatanova and Thakar, 2008). N-terminal acetylations are required for proper transcription, which are recognized by bromodomain containing transcription factor (Giaimo et al., 2019; Kim et al., 2009; Olson et al., 2020). The substitution from NK of H2A to DS/T of H2A.Z in docking domain enhances the acidity of H2A.Z nucleosome surface (Suto et al., 2000) and enhances chromatin compaction (Fan et al., 2004). H2A.Z nucleosome has long L1 loop, which is located at the surface of H2A.Z-H2A.Z interaction (Horikoshi et al., 2016; Suto et al., 2000). Thus, long L1 loop causes steric effects and destabilizes H2A.Z nucleosome *in vitro* (Horikoshi et al., 2016). These features diversify the functions of chromatin, as H2A.Z is essential for viability in many organisms, including *Drosophila melanogaster* (Daal and Elgin, 1992), *Tetrahymena thermophiula* (Liu et al., 1996), and *Xenopus leavis* (Iouzalen et al., 1996), and has specific roles in gene regulation, chromosome segregation, DNA replication, DNA repair, and the stress response (Long et al., 2020; Talbert and Henikoff, 2014; Zlatanova and Thakar, 2008).

In many eukaryotes, H2A.Z is enriched at the +1 nucleosome, the first nucleosome after a transcriptional start site (TSS) (Buchanan et al., 2009; Giaimo et al., 2019; Zlatanova and Thakar, 2008). The chromatin remodeling SWR complex deposits H2A.Z-H2B dimer at nucleosomes in an ATP-dependent manner (Mizuguchi et al., 2004) (Figure 5A). While there are homotypic (H2A.Z-H2A.Z) and heterotypic (H2A.Z-H2A) H2A.Z containing nucleosome, 70-95 % of H2A.Z nucleosome are homotypic throughout cell cycle in trophoblast stem cells (Nekrasov et al., 2012). The localization of H2A.Z is well correlated with that of H3 and H4 acetylation (Buchanan et al., 2009). Bdf1, a component of SWR complex, binds NuA4- and GCN5-mediated histone acetylation though its bromodomain and recruits SWR complex to promoter region for H2A.Z deposition (Altaf et al., 2010; Buchanan et al., 2009; Raisner et al., 2005; Zhang et al., 2005). Moreover, Swc2, a component of

SWR complex recognizes naked DNA at nucleosome free region of promoter, which can also recruit SWR complex (Ranjan et al., 2013; Yen et al., 2013).

H2A.Z enhances nucleosome barrier activity (Chen et al., 2019) and is required for Pol II proximal pausing (Mylonas et al., 2021) (Figure5B). Furthermore, H2A.Z is required for bivalent gene repression in embryonic stem cells, contributing to accurate differentiation (Creyghton et al., 2008). Furthermore, H2A.Z is removed from the +1 nucleosome at the time of transcriptional initiation (Ranjan et al., 2020; Tramantano et al., 2016), suggesting that H2A.Z has a negative effect on transcription (Figure 5B). Indeed, in fission yeast and budding yeast, the enrichment of the H2A.Z at TSS of euchromatic genes negatively corelates with expression levels (Buchanan et al., 2009; Guillemette et al., 2005; Zhang et al., 2005; Zofall et al., 2009).

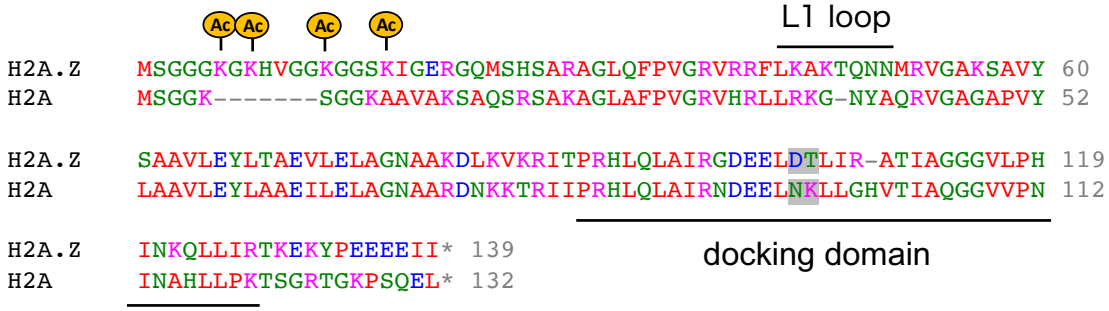

Figure 4 alignment of fission yeast H2A.Z and H2A
Fission yeast H2A.Z/Pht1 and H2A/Hta1 are aligned. N-terminus of H2A.Z and H2A are greatly different. Acetylation of N-terminus Lysins of H2A.Z is well conserved modification, which is required for proper transcription. H2A.Z has unique residues in L1 loop and docking domain; L1 loop is located at the surface of H2A.Z-H2A.Z interaction, and docking domain interacts with H3-H4 dimer. H2A.Z has long L1 loop, which decreases nucleosome stability *in vitro*. Docking domain of H2A.Z is substituted to acidic residues, which is required for chromatin compaction *in vitro*.

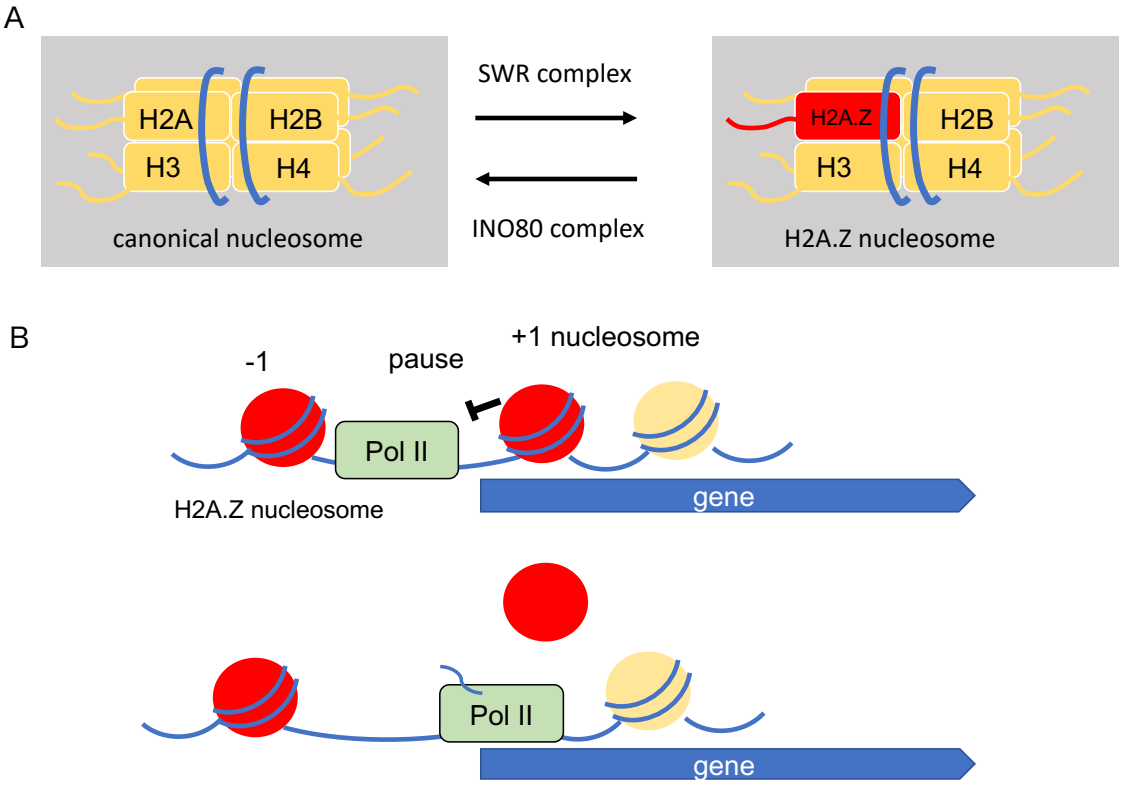

Figure 5 functions of H2A.Z at TSS

A) Illustrations of canonical nucleosome and H2A.Z containing nucleosome. SWR complex integrates H2A.Z-H2B dimer and evicts canonical nucleosome in an ATP-dependent manner. By contrast, INO80 complex evicts H2A.Z-H2B dimer and integrates H2A-H2B dimer in an ATP-dependent manner.

B) In euchromatin, H2A.Z are highly enriched at transcription start site (TSS) of euchromatic gene. H2A.Z nucleosome is required for Poll II pausing. At the time of transcription, H2A.Z nucleosome is disassembled by transcription itself or preinitiation complex assembly.

1-4 Silencing roles of H2A.Z

While H2A.Z is not highly enriched at the heterochromatic region, loss of DNA methylation and/or H3K9me increases the deposition of H2A.Z at heterochromatic regions in mammals and *Arabidopsis thaliana* (Boyarchuk et al., 2014; Saksouk et al., 2014; Zilberman et al., 2008). However, this deposition mechanism, and the role for accumulating H2A.Z at defective heterochromatin, are still unknown. It has been reported that H2A.Z has been shown to enhance nucleosome compaction (Fan et al., 2004; Zlatanova and Thakar, 2008). Loss of Pht1, an orthologue of H2A.Z in fission yeast leads to the de-repression of subtelomeric silencing, without affecting H3K9me (Zofall et al., 2009), and activates the expression of transposable elements (Anver et al., 2014). However, detailed silencing mechanisms for Pht1 are still unknown.

1-5 This study

In this study, I identify novel functions of Pht1 at heterochromatin. The amount of Pht1 present in pericentromeric heterochromatin is lower than at euchromatic gene promoters, and once H3K9me is decreased by the loss of Clr4 or Dcr1, Pht1 becomes enriched in a SWR-dependent manner. I find that this Pht1 accumulation in *dcr1*Δ cells suppresses the demethylation activity of Epe1 to maintain a certain level of H3K9me. Moreover, I show that loss of Pht1 in *clr4*Δ cells represses ncRNA transcription, possibly through a mechanism similar to the Pht1-dependent control of euchromatic genes. These results suggest that fission yeast H2A.Z plays multiple functions to compensate for defects in heterochromatin.

2. Experimental Procedures

2-1 Strains and media

The *S. pombe* strains used in this study are listed in Table 1. Construction of strains was performed as previously described (Sabatinos and Forsburg, 2010). For gene deletion, target gene ORFs were replaced with drug resistance gene cassettes: kanMX6, hphMX6, and natMX6, which confer resistance to G418 (Wako), hygromycin B (Wako), and nourseothricin (clonNAT, WERNER BioAgents), respectively. For the construction of tagged strains, drug resistance gene were inserted downstream or upstream of the ORF. For Pht1-4myc strains, DNA cassettes were amplified from FY32087 (NBRP) and transformed into the relevant strains. For Pht1ΔN-4myc, Pht1(4KQ)-4myc, and Pht1(4KR)-4myc strains, DNA cassettes were amplified from FY32471 (NBRP), FY32472 (NBRP), and FY32473 (NBRP), respectively, and fused to the myc-tag sequence by fusion PCR methods. For Epe1 OP strains, the sequence of the *urg1* promoter and 3xflag were inserted at the N-terminus of Epe1, as previously described (Sorida et al., 2019). It is worth noting that the expression of the gene controlled by *urg1* promoter is highly expressed in the presence of uracil (Watson et al., 2011). All tagged strains were confirmed by sequence analysis and western blotting.

Table 1 list of strains used in this study

name	genotype	mating type	source
FY2002	ade6-DN/N leu1-32 ura4-DS/E imr1L::ura4+ otr1R::ade6+	h+	gift from R. Allshire
KFY174	ade6-DN/N leu1-32 ura4-DS/E imr1L::ura4+ otr1R::ade6+, clr4Δ::natMX, pht1:4myc::KanMX	h+	this study
KFY191	leu1-32 ade6-DN/N, ura4-DS/E, ura4-DS/E imr1L::ura4+, otr1R::ade6+,hphMX6::Purg1::3FLAG::epe1, pht1::4myc::KanMX	h+	this study
KFY248	ade6-DN/N leu1-32 ura4-DS/E imr1L::ura4+ otr1R::ade6+, pht1:4myc::KanMX	h+	this study
KFY468	ade6-DN/N leu1-32 ura4-DS/E imr1L::ura4+ otr1R::ade6+, pht1:4myc::KanMX dcr1Δ::hphMX	h+	this study
KFY215	ade6-DN/N leu1-32 ura4-DS/E imr1L::ura4+ otr1R::ade6+, swi6Δ::natMX pht1-4myc::KanMX	h+	this study
KFY257	ade6-DN/N leu1-32 ura4-DS/E imr1L::ura4+ otr1R::ade6+, pht1:4myc::KanMX swr1Δ::hphMX	h+	this study
KFY295	ade6-DN/N leu1-32 ura4-DS/E imr1L::ura4+ otr1R::ade6+, clr4Δ::natMX, pht1:4myc::KanMX swr1Δ::hphMX	h+	this study
KFY368	ade6-DN/N leu1-32 ura4-DS/E imr1L::ura4+ otr1R::ade6+, pht1:4myc::KanMX bdf1Δ::hphMX	h+	this study
KFY373	ade6-DN/N leu1-32 ura4-DS/E imr1L::ura4+ otr1R::ade6+, clr4Δ::natMX, pht1:4myc::KanMX bdf1Δ::hphMX	h+	this study
KFY72	ade6-DN/N leu1-32 ura4-DS/E imr1L::ura4+ otr1R::ade6+, pht1Δ::hphMX6	h+	this study
KFY177	ade6-DN/N leu1-32 ura4-DS/E imr1L::ura4+ otr1R::ade6+, clr4Δ::natMX	h+	ABN075 our stock
KFY194	ade6-DN/N leu1-32 ura4-DS/E imr1L::ura4+ otr1R::ade6+ clr4Δ::natMX pht1Δ::KanMX	h+	this study
KFY178	ade6-DN/N leu1-32 ura4-DS/E imr1L::ura4+ otr1R::ade6+, swi6Δ::natMX	h+	this study
KFY179	ade6-DN/N leu1-32 ura4-DS/E imr1L::ura4+ otr1R::ade6+, swi6Δ::natMX, pht1Δ::KanMX	h+	this study
KFY465	ade6-DN/N leu1-32 ura4-DS/E imr1L::ura4+ otr1R::ade6+, dcr1Δ::hphMX	h+	this study
KFY502	ade6-DN/N leu1-32 ura4-DS/E imr1L::ura4+ otr1R::ade6+, dcr1Δ::hphMX pht1Δ::KanMX	h+	this study
KFY111	ade6-DN/N leu1-32 ura4-DS/E imr1L::ura4+ otr1R::ade6+, swr1Δ::hphMX6	h+	this study
KFY245	ade6-DN/N leu1-32 ura4-DS/E imr1L::ura4+ otr1R::ade6+ clr4Δ::natMX swr1Δ::hphMX	h+	this study
KFY275	ade6-DN/N leu1-32 ura4-DS/E imr1L::ura4+ otr1R::ade6+, clr4Δ::natMX pREP-5FALG-Clr4+(Leu2)	h+	this study
KFY279	ade6-DN/N leu1-32 ura4-DS/E imr1L::ura4+ otr1R::ade6+ clr4Δ::natMX pht1Δ::KanMX pREP-5FALG-Clr4+(Leu2)	h+	this study
KFY283	ade6-DN/N leu1-32 ura4-DS/E imr1L::ura4+ otr1R::ade6+ clr4Δ::natMX pht1Δ::KanMX pREP1	h+	this study
KFY288	ade6-DN/N leu1-32 ura4-DS/E imr1L::ura4+ otr1R::ade6+ pREP1(Leu2)	h+	this study
KFY318	ade6-M210 his2 leu1-32 ura4DS/E Kint2::ura4+ dcr1Δ::hphMX6	h90	SS908 our stock
KFY319	ade6-M210 his2 leu1-32 ura4DS/E Kint2::ura4 clr4Δ::hphMX6	h90	SS872 our stock
KFY320	ade6-M210 his2 leu1-32 ura4DS/E Kint2::ura4 clr4Δ::hphMX6 pht1Δ::kanMX	h90	this study
KFY321	ade6-M210 his2 leu1-32 ura4DS/E Kint2::ura4+ pht1Δ::kanMX	h90	this study
KFY580	ade6-M210 his2 leu1-32 ura4DS/E Kint2::ura4+ dcr1Δ::hphMX6 pht1Δ::KanMX	h90	this study
KFY581	ade6-M210 his2 leu1-32 ura4DS/E Kint2::ura4+ dcr1Δ::hphMX6 pht1Δ::KanMX	h90	this study
KFY588	h90 leu1-32 ade6-m210 ura4-DS/E Kint2::ura4+	h90	HKV174 our stock
KFY626	h+ leu1-32 ade6-DN/N,ura4-DS/E , ura4-DS/E imr1L::ura4+, otr1R::ade6+ Δepe1::kanMx6,Δdcr1::hphMX6	h+	AKB004 our stock
KFY642	h+ leu1-32 ade6-DN/N,ura4-DS/E , ura4-DS/E imr1L::ura4+, otr1R::ade6+ Δepe1::kanMx6,Δdcr1::hphMX6 pht1Δ::natMX	h+	this study
KFY643	h+ leu1-32 ade6-DN/N,ura4-DS/E , ura4-DS/E imr1L::ura4+, otr1R::ade6+ Δepe1::kanMx6,Δdcr1::hphMX6 pht1Δ::natMX	h+	this study
KFY182	leu1-32 ade6-DN/N, ura4-DS/E, ura4-DS/E imr1L::ura4+, otr1R::ade6+,hphMX6::Purg1::3FLAG::epe1	h+	this study
KFY195	leu1-32 ade6-DN/N, ura4-DS/E, ura4-DS/E imr1L::ura4+, otr1R::ade6+,hphMX6::Purg1::3FLAG::epe1, pht1Δ::KanMX	h+	this study
KFY2	ade6-DN/N leu1-32 ura4-DS/E imr1L::ura4+ otr1R::ade6+, epe1Δ::KanMX	h+	this study
KFY81	ade6-DN/N leu1-32 ura4-DS/E imr1L::ura4+ otr1R::ade6+, epe1Δ::KanMX,, pht1Δ::hphMX6	h+	this study
KFY3	leu1-32 ade6-DN/N, ura4-DS/E, imr1L::ura4+, otr1R::ade6+, ⊿epe1::3FLAG-Epe1::KanMX	h+	this study
KFY666	leu1-32 ade6-DN/N, ura4-DS/E, imr1L::ura4+, otr1R::ade6+, ⊿epe1::3FLAG-Epe1::KanMX pht1Δ::natMX	h+	this study
KFY449	ade6-DN/N leu1-32 ura4-DS/E imr1L::ura4+ otr1R::ade6+,pht1(4KQ)-4myc::kanMX	h+	this study
KFY450	ade6-DN/N leu1-32 ura4-DS/E imr1L::ura4+ otr1R::ade6+,clr4Δ::natMX, pht1ΔN-4myc::kanMX	h+	this study
KFY451	ade6-DN/N leu1-32 ura4-DS/E imr1L::ura4+ otr1R::ade6+,clr4Δ::natMX, pht1(4KR)-4myc::kanMX	h+	this study
KFY453	ade6-DN/N leu1-32 ura4-DS/E imr1L::ura4+ otr1R::ade6+,clr4Δ::natMX, pht1(4KO)-4myc::kanMX	h+	this study
KFY454	ade6-DN/N leu1-32 ura4-DS/E imr1L::ura4+ otr1R::ade6+,pht1ΔN-4myc::kanMX	h+	this study
KFY460	ade6-DN/N leu1-32 ura4-DS/E imr1L::ura4+ otr1R::ade6+,pht1(4KR)-4myc::kanMX	h+	this study
KFY145	ade6-DN/N leu1-32 ura4-DS/E imr1L::ura4+ otr1R::ade6+ rrp6::13myc::natMX	h+	SS216 our stock
KFY541	ade6-DN/N leu1-32 ura4-DS/E imr1L::ura4+ otr1R::ade6+ rrp6::13myc::natMX clr4Δ::KanMX	h+	EOS747 our stock
KFY542	ade6-DN/N leu1-32 ura4-DS/E imr1L::ura4+ otr1R::ade6+ rrp6::13myc::natMX dcr1Δ::hphMX	h+	EOS739 our stock
KFY561	ade6-DN/N leu1-32 ura4-DS/E imr1L::ura4+ otr1R::ade6+ rrp6::13myc::natMX pht1Δ::KanMX	h+	this study
KFY567	ade6-DN/N leu1-32 ura4-DS/E imr1L::ura4+ otr1R::ade6+ rrp6::13myc::natMX dcr1Δ::hphMX pht1Δ::KanMX	h+	this study
KFY540	h+, ade6-DN/N, leu1-32, ura4-DS/E, imr1L::ura4+, otr1R::ade6+, Δrrp6::kanMX6	h+	ss220 our stock
KFY552	h+, ade6-DN/N, leu1-32, ura4-DS/E, imr1L::ura4+, otr1R::ade6+, Δrrp6::kanMX6 clr4Δ::hphMX	h+	this study
KFY571	h+, ade6-DN/N, leu1-32, ura4-DS/E, imr1L::ura4+, otr1R::ade6+, Δrrp6::kanMX6 dcr1Δ::hphMX	h+	this study
KFY382	wildtype L972	h-	SFY397 our stock
A2730	h+ ura4::[4xTetO-ade6] his3D ade6-DNN leu1:nmt81xTetR"off"-2xFLAG-clr4-cdd	h?	gift from R. Allshire
KFY592	h+ ura4::[4xTetO-ade6] his3D ade6-DNN leu1:nmt81xTetR"off"-2xFLAG-clr4-cdd epe1Δ::natMX	h?	RS636 our stock
KFY606	h+ ura4::[4xTetO-ade6] his3D ade6-DNN leu1:nmt81xTetR"off"-2xFLAG-clr4-cdd epe1Δ::natMX pht1Δ::KanMX	h?	this study
KFY615	h+ ura4::[4xTetO-ade6] his3D ade6-DNN leu1:nmt81xTetR"off"-2xFLAG-clr4-cdd pht1Δ::KanMX	h?	this study
KFY681	ade6-DN/N leu1-32 ura4-DS/E imr1L::ura4+ otr1R::ade6+,pht1ΔN-myc::kanMX dcr1Δ::hphMX	h+	this study

2-2 Spot assay

Fresh yeast cells grown on rich media were resuspended in sterilized water in a 96-well plate and serially diluted, and then 5 µl of dilutions were spotted onto the indicated media. Cells were incubated at 30 °C for 3 days and photographed.

2-3 Western blotting

Cells were cultured in 10 ml of YES media to 1x10^7 cells/ml. Cells were harvested by centrifugation and stored at -80 °C. Cell pellets were resuspended in 200 µl of 1x laemmli buffer (4 M urea, 2% SDS, 0.06 M Tris-HCl pH 6.8, 10% glycerol, and 0.3 M β-mercaptoethanol) and incubated at 95 °C for 5 min. Zirconia beads were added, and the cells were disrupted using a multi beads shocker (yasui kikai) with 10 cycles of 60 sec ON and 60 sec OFF. The resulting whole cell extracts were boiled at 95 °C for 5 min and centrifuged at 15 000 rpm for 5 min, and the supernatants were collected for use in downstream processes. Proteins were separated by SDS-PAGE and transferred to PVDF membrane (Merk Millipore). Membranes were blocked in 1% skim milk and incubated in primary antibody, diluted in Can Get Signal (TOYOBO) according to the manufacturer's protocol, overnight at 4 °C. Antibodies used for Western blotting are as follows: anti-Myc (4A6, Merck Millipore), anti-H3CT pan (Merck Millipore), and anti-tubulin (B-5-1-2, Sigma-Aldrich). Membranes were incubated with horseradish peroxidase-conjugated anti-mouse IgG or anti-rabbit IgG (GE Healthcare) for 60 min at room temperature, and images were captured using an Amersham ImageQuant 800 (GE Healthcare).

2-4 ChIP-qPCR

Yeast strains were cultured in 50 ml of YES media to 1x10^7 cells/ml, fixed with 1% formaldehyde (nacarai tesque) for 30 min, and quenched by the addition of 125 mM glycine. Cells were harvested and stored at -80 °C until needed. Cell pellets were re-suspended in ChIP buffer (50 mM HEPES-KOH pH 7.5, 140 mM NaCl, 1 mM EDTA, 1% Triton X-100 (nacalai tesque), 0.1% Na-Deoxycholate (Merk Millipore)) containing 1 mM PMSF and 1x protease inhibitor cocktail (0.25 mg/L bestatin, 15 mg/L benzamidine HCl, 0.25 mg/L pepstatin A, and 0.25 mg/L leupeptin), and disrupted with zirconia beads using a multi beads shocker (yasui kikai). Whole cell extracts were centrifuged at 15 000 rpm for 60 min. The

supernatant was removed, and the chromatin-containing pellet was resuspended in ChIP buffer. Chromatin was digested by sonication using a Bioruptor UCW-310 (Cosmo Bio) with 15 cycles of 30 sec ON and 30 sec OFF under 10 °C. The extracts were centrifuged at 15 000 rpm for 5 min and the supernatants were used as the input of immunoprecipitation (IP). Before IP, Dynabeads M-280 Sheep anti-mouse or anti-rabbit IgG (Invitrogen) were incubated with 1 µg of the following antibodies for 3–4 hours, and washed once with ChIP buffer: anti-H3K9me (5.1.1, mAbProtein Co.), anti-Myc (4A6, Merck Millipore), anti-Ser2 phosphorylated Rpb1 (a kind gift form H. Kimura, Tokyo Institute of Technology), anti-H3CT pan (Merck Millipore), and anti-FLAG antibody (M2, Sigma-Aldrich). Note that the anti-H3K9me antibody recognizes H3K9me1, me2, and me3. The beads were incubated with 100 µl of extract for 2 hrs at 4 °C and washed twice with ChIP buffer, twice with High Salt buffer (ChIP buffer containing 500 mM NaCl), and twice with LiCl buffer (10 mM Tris pH 8.0, 0.25 M LiCl, 0.5% NP-40, 0.5% Na-Deoxycholate, and 1 mM EDTA). The beads were subsequently incubated with reverse cross link buffer (20 mM tris pH 7.6, 1 mM EDTA, 0.8% SDS) containing 0.1 mg/ml RNase A for 30 min at 37 °C, and incubated with 0.2 mg/ml Protease K for 60 min at 55 °C. DNA cross linking was reversed by incubating at 95 °C for 12 min. For input samples, one tenth of input was treated with RNase and ProK, and cross links were reversed. DNA was purified using FastGene Gel/PCR Extraction Kit (NIPPON Genetics). Both IP and input DNA samples were quantified by real-time PCR LC96 (Roche Life Science). Primers are listed in Table 2.

Table 2 list of primers used in this study

KF	name	sequence	used for
63	dh F	tcagcagtccttgggaaatg	ChIP, RT
64	dh R	gatgcccatgttcattccac	ChIP, RT
134	dg F	CTGCGGTTCACCCTTAACATC	ChIP, RT
135	dg R	CAACTGCGGATGGAAAAAGT	ChIP, RT
152	cenH dh F	GCTAAGATCGATTGGTGACG	ChIP, RT
153	cenH dh R	AAGTTCACTGTTCTTATACACTGG	ChIP, RT
221	nda2 F2	TCGCCGAAATCTTGACATTG	ChIP, RT
222	nda2 R2	AATACGAGGGTATGGCACAAG	ChIP, RT
225	tlh1-tlh2 F	ATGGTCGTCGCTTCAGAAATTGC	ChIP, RT
226	tlh1-tlh2 R	CTCCTTGGAAGAATTGCAAGCCTC	ChIP, RT
219	ura4 F	GAATGGTTTGAGAAGCATACC	ChIP, RT
220	ura4 R	GAGTACGATATTGCTGTCCC	ChIP, RT
258	gfr2 F	AGGCTGTATTCCCAACATCC	ChIP
259	gfr2 R	ATGCCTTCTTCTTCTTCTCAG	ChIP
335	vid21 pro F	AGAACAAGCGATTTCTCCGAGC	ChIP
336	vid21 pro R	GGGATTTGAGCCCGCAATCA	ChIP
337	vid21 orf F	AACCTTTAGTGTGCGGCCTC	ChIP
338	vid21 orf R	ACAAACCTGGTGGTGTTAACCT	ChIP
356	tub1	GTACTGGCCCATACCGTGAT	RT
357	tub1	CGAATGGAAGACGAGAAAGC	RT
384	mtDNA F	ACCAGTACACGAACACGCATT	ChIP
385	mtDNA R	ATCCTTCAATCTCCCTCTCCA	ChIP
392	clr4 qpcr F	ACTGCGGGAAATTGAAGGAC	RT
393	clr4 qpcr R	GAGCAATTGCATCCAGATTG	RT
394	sir2 qocr F	AAACGTGAGGTTGCTAGGAG	RT
395	sir2 qpcr R	CCAAACTTGTACTTATGCCT	RT
396	rrp6 qpcr F	ACTGAAGCTGCAAACCCGAG	RT
397	rrp6 qpcr R	CTATGGGGTTTGAGGGTTCT	RT
398	dhp1 qpcr F	TACATCCGCTGACGCCCTTC	RT
399	dhp1 qpcr R	TCTTCTGGGGTTAACACCCT	RT
370	nam7 R	ATGCCCATGTTCATTCCACT	RT
372	nam7L R	GCCTTTAAATGACCGCACTAA	RT
373	nam7 F	TGGCTATGATTGGAAGGTTG	RT

2-5 RT-qPCR

Cells were cultured in 15 ml of YES to 1x10^7 cell/ml, harvested by centrifugation, and stored at -80 °C. For total RNA extraction, cells were incubated with an equal volume of acid phenol and AE buffer (50 mM sodium acetate (pH 5.2), 10 mM EDTA, and 1% SDS) at 65 °C for 60 min. Total RNA was precipitated by EtOH precipitation and treated with 10 U of DNase I (Takara Bio) for 60 min at 37 °C. DNase I was removed by phenol/chloroform extraction, and 1 μg of total RNA was reverse transcribed with PrimeScript Reverse Transcriptase (Takara Bio) using an oligo dT(15) primer, according to the manufacturer's protocol. For Figure S3, *nam7*, *nam7-L*, *tub1*$^{+}$ reverse primers were used. cDNAs were quantified by real-time PCR LC96 (Roche Life Science). Standard curves were created using serial dilutions of cDNA from *clr4*Δ*pht1*Δ cells. Expression levels relative to *nda2*$^{+}$ were determined by dividing cDNA concentrations for each gene by *nda2*$^{+}$ (tubulin). RT- samples, which were equally reacted without reverse transcriptase, were also quantified, but signals were outside the range covered by the standard curve. Primers were listed in Table 2.

2-6 Clr4 reintroduction

For the construction of Clr4 expression plasmids, DNA fragments containing *5xflag-clr4*$^{+}$ and the *clr4*$^{+}$ promoter and terminator sequences were amplified from SPM1145 (Sadaie et al., 2004) and inserted into the PstI/XmaI sites of pREP1 as previously reported (Gerace et al., 2010), noting that *nmt1* promoter was removed by PstI/XmaI digestion. *pclr4*$^{+}$ was introduced into *clr4*Δ and *clr4*Δ*pht1*Δ cells. Expression of Clr4 was confirmed by western blotting. pREP1 was also introduced as a negative control. For ChIP analysis, cells were cultured in EMM lacking leucine.

2-7 TetR-Clr4 mediated heterochromatin silencing assay

A strain containing *pnmt81-tetR-clr4* and *4xtetO-ade6* was a gift from R. Allshire (Audergon et al., 2015). Cells were cultured in PMG liquid media overnight before being serially diluted and spotted onto PMG low ade (7.5 mg/L adenine) plates with or without 10 μM anhydrotetracycline and 5 mg/L thiamin (+AHT and -AHT, respectively). Plates were incubated at 30 °C for 5 days and images were captured.

3. Results

3-1 loss of H3K9me induces Swr1-mediated H2A.Z deposition at the pericentromeric heterochromatin.

3-1.1 Loss of H3K9me induces H2A.Z deposition at the pericentromeric heterochromatin.

Since localization of H2A.Z negatively corelates with that of H3K9me in many organisms (Boyarchuk et al., 2014; Zilberman et al., 2008), I first investigated whether Pht1, an orthologue of H2A.Z in fission yeast accumulates at pericentromeric heterochromatin in mutants that exhibit decreased levels of H3K9me (Figure 6A). As previously observed (Hou et al., 2010), Pht1 was highly enriched at the transcription start site (TSS) of the euchromatic gene, *vid21*$^{+}$. Lower but significant levels of enrichment were observed at the *vid21*$^{+}$ open-reading frame (ORF), as they were higher than those for mitochondrial DNA, where Pht1is not supposed to exist (Figure 6B). In wild-type cells, Pht1 localization at the pericentromere and the *vid21*$^{+}$ ORF were similar. H3K9me were highly occupied at *dg* and *dh* heterochromatic region compared to control locus, euchromatic gene *nda2*$^{+}$ (Figure 7A). In *clr4Δ* cells, in which H3K9 methylation was abolished (Figure 7A), Pht1 enrichment was increased approximately 1.5- and 4-fold at the *dg* and *dh* region, respectively (Figure 6A). I also detected a modest increase in Pht1 localization at the pericentromere in *dcr1Δ* cells (Figure 6A), in which total H3K9me was reduced to approximately 50% of the wild type (Figure 7A). These results are consistent with the previous suggestion that H2A.Z deposition negatively correlates with that of H3K9me.

A decrease in H3K9me results in increased transcription at heterochromatin. To exclude the possibility that increased transcription in *dcr1*Δ or *clr4*Δ cells induced Pht1 deposition, I examined Pht1 localization in *swi6*Δ cells and cells over-producing *epe1*$^{+}$ (*epe1* OP) using *urg1* promoter, which had reduced levels of heterochromatic silencing but did not significantly affect H3K9me levels (Figure 7A and B). Pht1 did not accumulate at the pericentromere in these mutants (Figure 6A).

These data suggest that loss of H3K9me, and not transcriptional de-repression, induced Pht1 accumulation at the pericentromeric region.

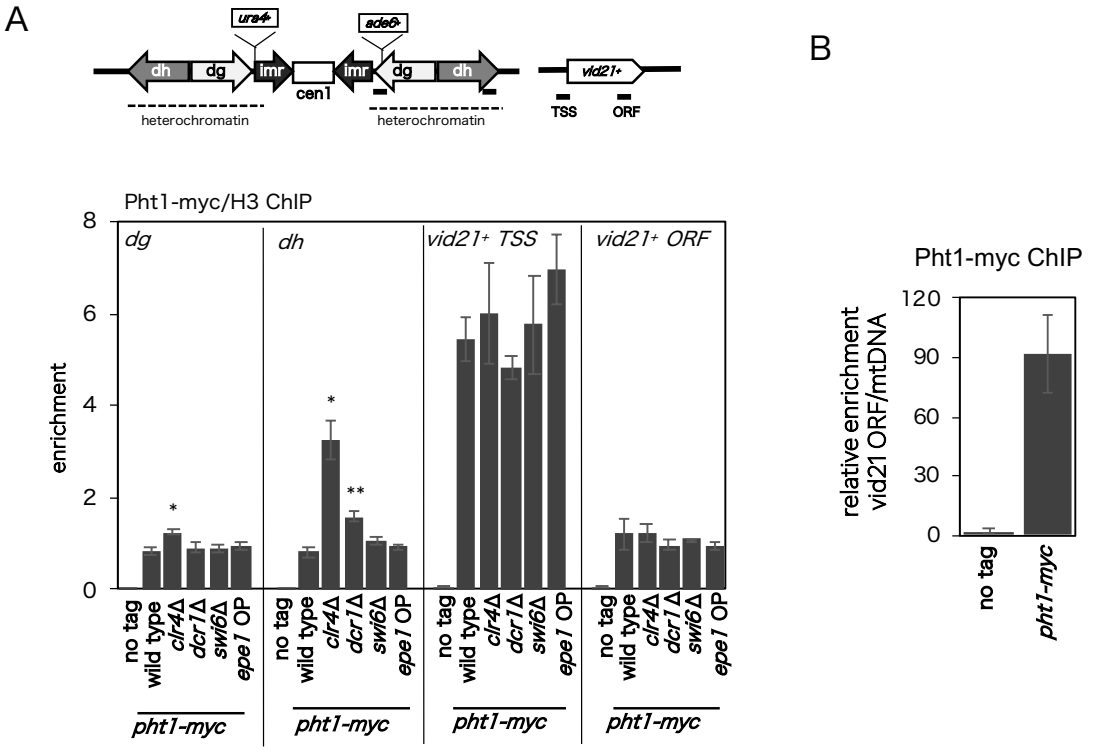

Figure 6 localizations of H2A.Z at pericentromere and euchromatic gene.

A) Schematic of the chromosome 1 centromere. *ura4*$^+$ and *ade6*$^+$ marker genes were inserted in *imr* (*imr*::*ura4*$^{+)}$ and *dg* (*otr*::*ade6*$^+$) repetitive elements, respectively. Black bars indicate the location of primers used in the following experiments. The primers of *dg* and *dh* are located ate siRNA hot spot. Localization of Pht1-myc relative to histone H3 was analyzed by chromatin immunoprecipitation quantitative PCR (ChIP-qPCR). *dg*, *dh*, and the transcription start site (TSS) and ORF of euchromatic gene *vid21*$^+$ are shown.

B) Localization of Pht1-myc at *vid21*$^+$ ORF relative to mtDNA analyzed by ChIP-qPCR. Data points and error bars represent the mean±SD of three independent experiments. p-values were calculated by two-tailed Student's t-test; *p<0.05, **p<0.01, and ***p<0.001.

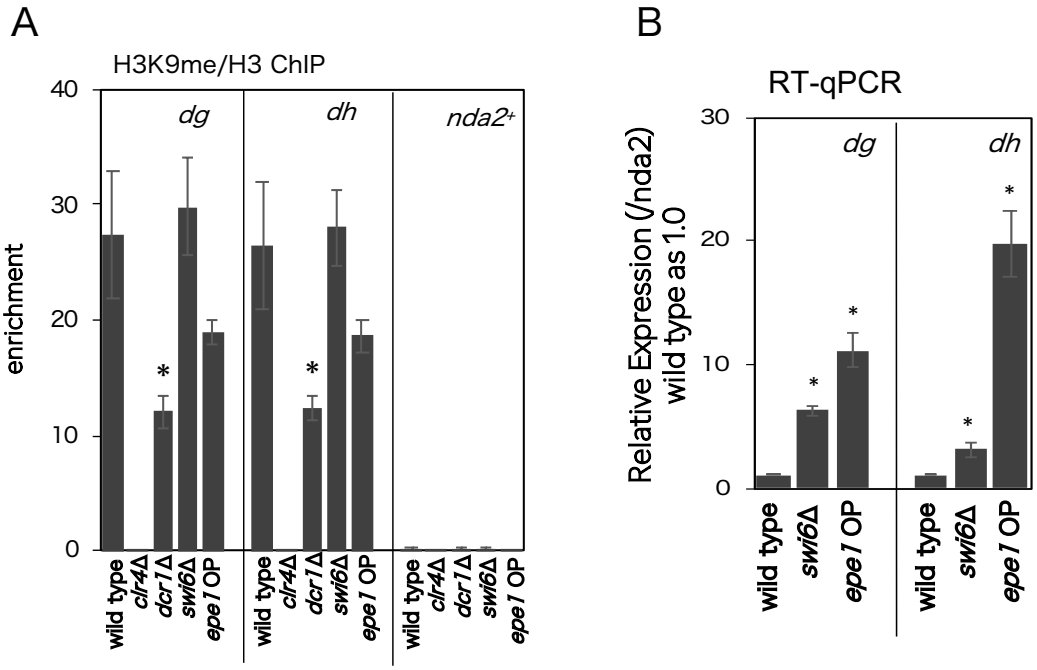

Figure 7 Effects of Clr4, Dcr1, Swi6 and Epe1 for heterochromatin assembly

A) Enrichment of H3K9me relative to H3 analyzed by ChIP-qPCR. The euchromatic gene *nda2*$^+$ was used as a negative control.

B) Expression of *dg* and *dh* measured by RT-qPCR. *nda2*$^+$ was used as a reference gene. Data points and error bars represent the mean±SD of three independent experiments. p-values were calculated by two-tailed Student's t-test; *p<0.05, **p<0.01, and ***p<0.001.

3-1.2 Swr1-mediated H2A.Z accumulation

The negative correlation between H2A.Z and H3K9me was well conserved but how H2A.Z is accumulation at heterochromatic region by loss of H3K9me was unclear. The chromatin remodeling SWR complex is known to integrate H2A.Z-H2B dimer into nucleosomes and is required for H2A.Z deposition at TSS (Mizuguchi et al., 2004). Swr1 is a catalytic subunit of the SWR complex, which exchanges H2A-H2B dimer for H2A.Z-H2B in an ATP-dependent manner. Thus, I next tested whether Pht1-accumulation is mediated by the SWR complex by ChIP-qPCR analysis using *swr1*$^{+}$ deletion mutants (Figure 8). As expected, deletion of *swr1*$^{+}$ decreased the level of Pht1 at the *vid21*$^{+}$ TSS. A slight decrease in Pht1 at *vid21*$^{+}$ ORF in *swr1*Δ cells suggested partial SWR complex-dependent incorporation. As shown previously (Buchanan et al., 2009), localization of Pht1 at the pericentromere did not change in *swr1Δ* cells. These results suggest that Swr1-independent H2A.Z deposition may function at the pericentromere. By contrast, the increase in Pht1 at the pericentromere observed in *clr4Δ* cells was disrupted in *clr4Δswr1Δ* cells (Figure 8), suggesting that the SWR complex is required for Pht1 accumulation in *clr4Δ* cells.

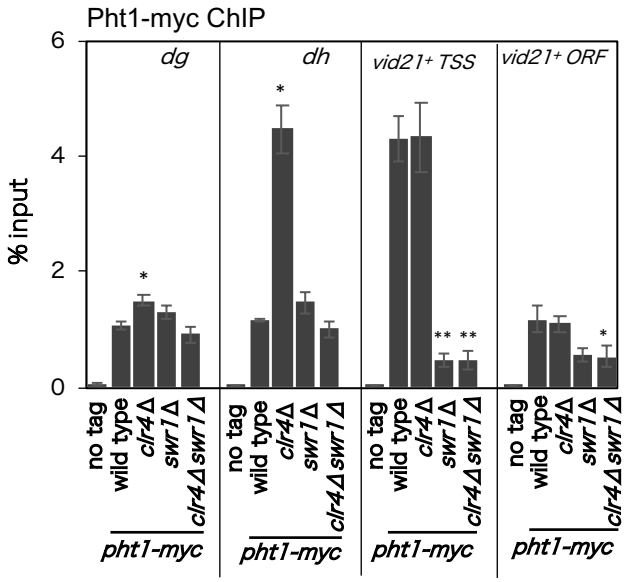

Figure 8 Swr1-mediated H2A.Z deposition at pericentromere and TSS of euchromatic gene.

A) Localization of Pht1-myc relative to histone H3 was analyzed by chromatin immunoprecipitation quantitative PCR (ChIP-qPCR). *dg*, *dh*, and the transcription start site (TSS) and ORF of euchromatic gene *vid21*$^{+}$ are shown. Data points and error bars represent the mean±SD of three independent experiments. p-values were calculated by two-tailed Student's t-test; *p<0.05, **p<0.01, and ***p<0.001.

3-1.3 Bdf1 is required for H2A.Z accumulation.

Next, I asked how the SWR complex deposits Pht1 in the absence of H3K9me. Since the SWR complex contains the bromodomain protein Bdf1, which recognizes acetylated histones (Buchanan et al., 2009; Hou et al., 2010), Swr1-dependent Pht1 enrichment correlates with H3K14ac and H4K16ac (Buchanan et al., 2009). Chromodomain protein Swi6 and Chp2 interacts with HDACs, which remove histone acetylation including H3K14ac (Motamedi et al., 2008). Thus, while histones are hypoacetylated in wild type heterochromatic regions, loss of *clr4*$^{+}$ increased H3K14 acetylation (Figure 9A). To investigate whether *bdf1*$^{+}$ is required for Swr1-mediated Pht1 deposition in *clr4Δ* cells, I measured Pht1 enrichment in *bdf1*$^{+}$ mutants using ChIP-qPCR (Figure 9B). Like *swr1Δ*, loss of Bdf1 decreased the accumulation of Pht1 at the pericentromere in *clr4Δ* cells; however, Pht1 enrichment at *vid21*$^{+}$ TSS was unaffected. The contribution of Bdf1 in Pht1 deposition at heterochromatin and euchromatin seems to be different. These results suggest that Bdf1 is required for Swr1-mediated Pht1 accumulation at pericentromeric heterochromatin when H3K9me is decreased. However, because Bdf1 recognizes acetyl-histone H3/H4 that acetylated at different positions (Ladurner et al., 2003), the acetylation required for this deposition is still unclear. Taken together, these data show that loss of H3K9me induces Swr1-dependent H2A.Z deposition at pericentromeres.

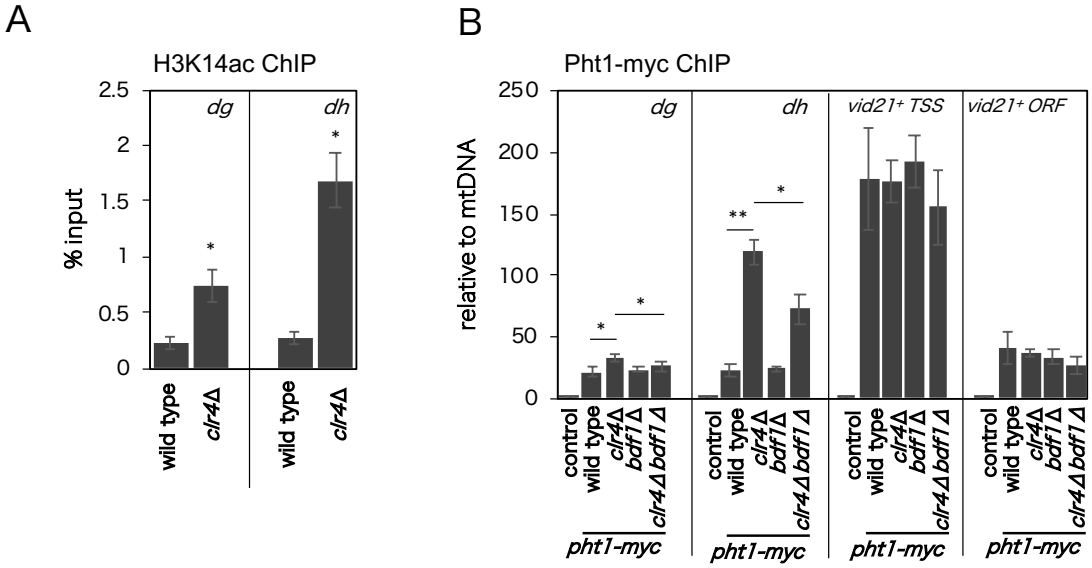

Figure 9 loss of Bdf1 abolishes H2A.Z accumulation at pericentromere.
A) Localization of H3K14ac relative was analyzed by chromatin immunoprecipitation quantitative PCR (ChIP-qPCR). *dg* and *dh* are shown.
B) Localization of Pht1-myc was analyzed by chromatin immunoprecipitation quantitative PCR (ChIP-qPCR). *dg*, *dh*, and the transcription start site (TSS) and ORF of euchromatic gene *vid21*$^{+}$ relative to mitochondrial DNA are shown. Data points and error bars represent the mean±SD of three independent experiments. p-values were calculated by two-tailed Student's t-test; *p<0.05, **p<0.01, and ***p<0.001.

3-2 H2A.Z represses pericentromeric ncRNA transcription at defective heterochromatin.

3-2.1 H2A.Z suppressed pericentric ncRNA transcription in *clr4*Δ and *dcr1*Δ cells.

To examine the effect of Pht1 accumulation at pericentromeric heterochromatin on the abundance of H3K9me, we measured ncRNA expression levels at the pericentromere by RT-qPCR in *pht1*$^{+}$ deletion mutants (Figure 10A). *pht1Δ* cells did not exhibit defects in silencing at the pericentromere, while in *clr4*Δ cells and *dcr1*Δ cells, I observed an increase in *dg/dh* expression, which corresponded with reduced H3K9me levels, as previously described (Volpe et al., 2002). A moderate increased *dg/dh* expression was observed in *swi6*Δ cells, whereas H3K9me did not change as previously observed (Nakayama et al., 2001). While *swi6*Δ*pht1*Δ cells did not alter *dg/dh* expression levels, epistatic silencing defects were observed in *clr4Δpht1Δ* and *dcr1Δpht1Δ* cells. It is worth noting that expression level of another reference gene, *tub1*$^{+}$ did not change in these mutants. These results suggest that Pht1 accumulating at the pericentromeric heterochromatin silences ncRNA expression in *clr4Δ* and *dcr1Δ* cells (Figure 6A). To distinguish whether Pht1-mediated silencing occurs during or post-transcription, I analyzed RNA polymerase II occupancy by ChIP-qPCR using an antibody against transcriptionally active Pol II (Figure 10B). This antibody recognizes the C-terminal repeat of Rpb1, the largest Pol II subunit, phosphorylated at the second serine, which represents elongating Pol II. Consistent with our RT-qPCR data, Pol II occupancy was increased in *clr4Δpht1Δ* and *dcr1Δpht1Δ* cells compared with *clr4Δ* and *dcr1Δ* single mutant, indicating that Pht1 represses heterochromatic transcription at low levels of H3K9me.

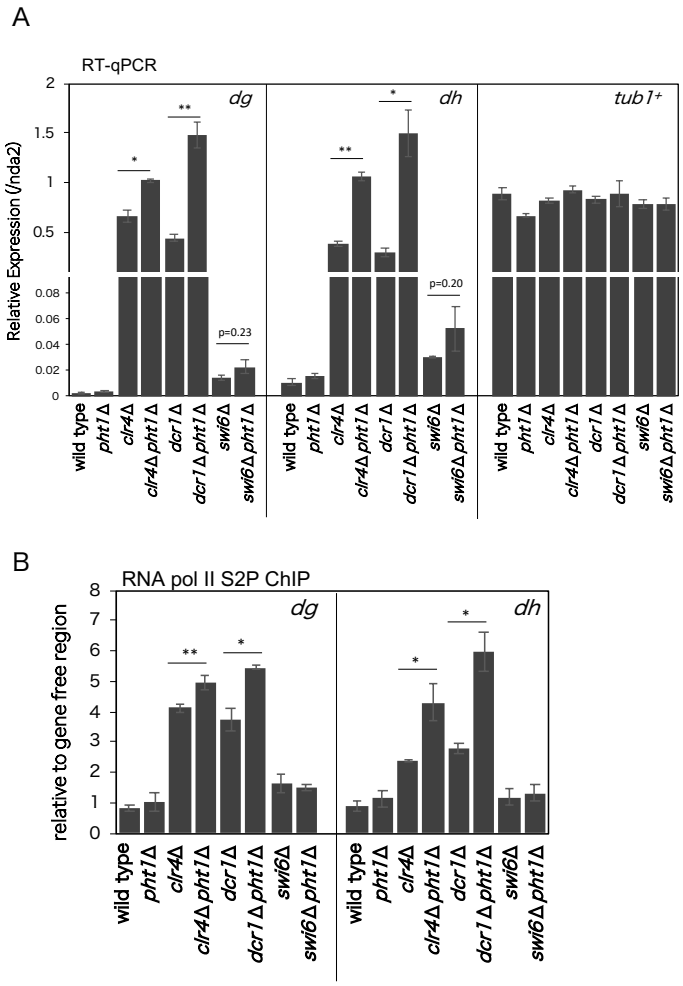

Figure 10 H2A.Z transcriptionally represses expression of pericentromeric ncRNA in *clr4*Δ and *dcr1*Δ cells.

A) Relative expression of *dg*, *dh*, and the reference gene *tub1*$^+$ were determined by RT-qPCR. Expression is normalized to *nda2*$^+$. B) Relative enrichment of Ser2 phosphorylated RNA polymerase II was analyzed by ChIP-qPCR. Each signal was normalized to the gene free region between *wis1* and *SPBC409.08*, where Pol II is depleted (Kato et al., 2013).

B) Relative expression levels of dg and dh were measured by RT-qPCR. *nda2*$^+$ was used as a reference gene. Data points and error bars represent the mean±SD of three independent experiments. p-values were calculated by two-tailed Student's t-test; *p<0.05, **p<0.01, and ***p<0.001.

3-2.2 Swr1 is partially required for transcriptional repression in *clr4*Δ cells.

Because Pht1 accumulates in *clr4Δ* cells in a SWR complex-dependent manner (Figure 8), I next analyzed the contribution that the SWR complex plays in Pht1-dependent silencing. RT-qPCR of ncRNA transcripts of *dg/dh* repeats showed that ncRNA expression levels in *clr4Δswr1Δ* cells were increased compared with *clr4Δ* cells (Figure 11), but this was less significant than in *clr4Δpht1Δ* cells. These results indicate that the Swr1-mediated Pht1 accumulation is partially required for Pht1-mediated silencing. Taken together, these data demonstrate that H2A.Z is actively incorporated into dysfunctional heterochromatic regions to suppress transcription.

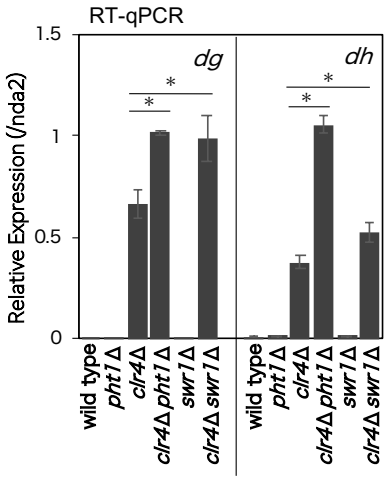

Figure 11 Swr1 is partially required for H2A.Z-mediated transcriptional repression in *clr4*Δ cells.

A) Relative expression levels of dg and dh were measured by RT-qPCR. *nda2*$^{+}$ was used as a reference gene. Data points and error bars represent the mean±SD of three independent experiments. p-values were calculated by two-tailed Student's t-test; *p<0.05, **p<0.01, and ***p<0.001.

3-3 H2A.Z facilitates RNAi-independent heterochromatin assembly.

3-3.1 H2A.Z is required for RNAi independent heterochromatin assembly at the pericentromere.

Although RNAi mutants significantly decrease H3K9me levels at pericentromeric heterochromatin, intermediate levels of H3K9me are maintained by an RNAi-independent pathway. Since loss of *pht1*$^{+}$ conferred synergistic silencing defects in *dcr1Δ* cells (Figure 10A), I hypothesized that *pht1*$^{+}$ is required for RNAi-independent H3K9 methylation, so I next examined H3K9me levels in these cells using ChIP-qPCR (Figure 12). *pht1Δ* cells exhibited a modest increase in H3K9me compared with wild-type cells, as previously described (Zofall et al., 2009). *dcr1Δ* cells retained 40% of H3K9me at both *dh* and *dg* repeats; however, the introduction of *pht1Δ* abolished H3K9me. *swi6*Δ*pht1*Δ cells did not change H3K9me level, which did not show synergistic silencing defects. These data suggest that *pht1*$^{+}$ is required for RNAi-independent heterochromatin maintenance.

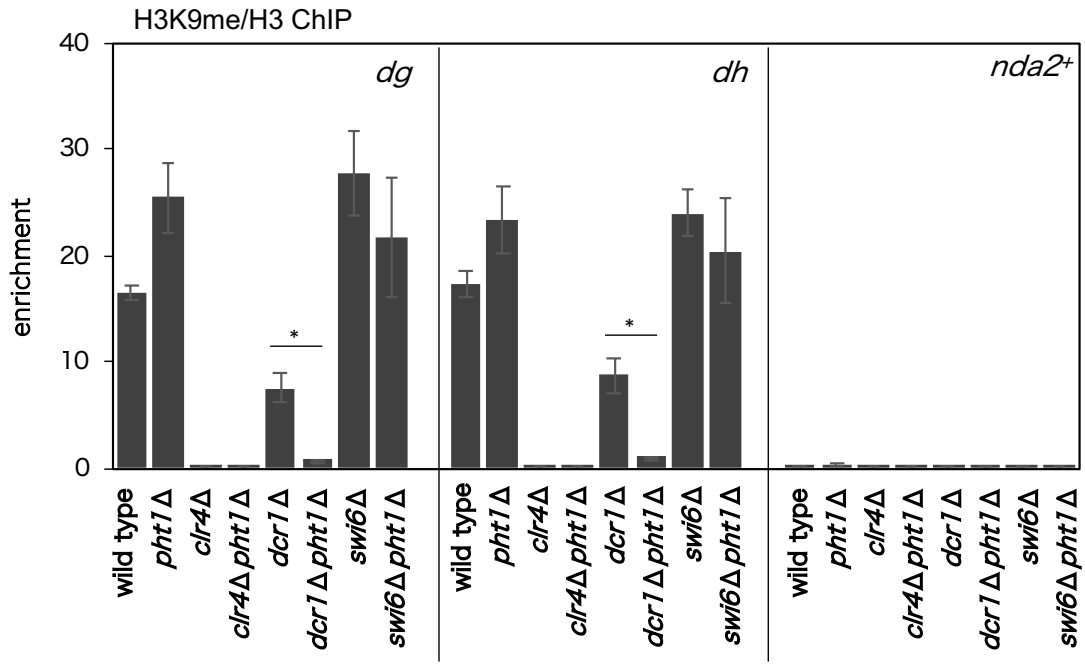

Figure 12 Loss of Pht1 abolishes RNAi-independent H3K9me in *dcr1*Δ cells at pericentromere.

Relative enrichment of H3K9me at *dg*, *dh*, and *nda2*$^{+}$ was analyzed by ChIP-qPCR. Enrichment was normalized to H3, and nda2+ was used as a negative control. Data points and error bars represent the mean±SD of three independent experiments. p-values were calculated by two-tailed Student's t-test: *p<0.05, **p<0.01, and ***p<0.001.

3-3.2 H2A.Z is not required for *de novo* heterochromatin formation.

ncRNAs transcribed from *dg* and *dh* repeats at the pericentromere target RNAi factors and provide substrates for siRNA synthesis during RNAi-dependent heterochromatin formation. Importantly, this RNAi-dependent system is required for *de novo* formation of heterochromatin (Hall et al., 2002). As described above, I saw no evidence that Pht1 is involved in RNAi-dependent heterochromatin formation; however, it was possible that regulation of ncRNA transcription by Pht1 in the absence of H3K9me may play a role in *de novo* formation of heterochromatin. To test this assumption, I reintroduced the *clr4*$^{+}$ gene, under a native promoter and terminator, into *clr4Δ* cells using *pclr4*$^{+}$ plasmids to test *de novo* heterochromatin formation (Figure 13). H3K9me was completely restored in *pht1Δ* cells, suggesting that suppression of ncRNA transcription by Pht1 in the absence of H3K9me is not required for the establishment of heterochromatin. As the establishment of heterochromatin is RNAi-dependent, these data support our suggestion that Pht1 is not involved in RNAi.

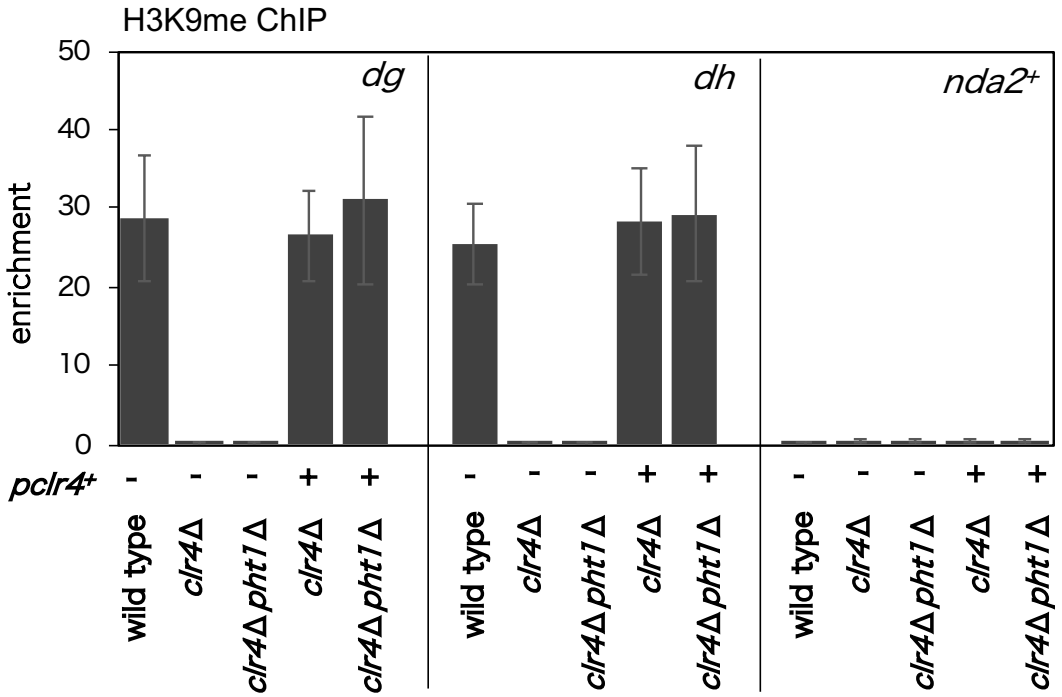

Figure 13 H2A.Z is not required for *de novo* heterochromatin formation. Enrichment of H3K9me was analyzed by ChIP-qPCR. *pclr4*$^{+}$ plasmid was introduced into *clr4*Δ strain and *clr4*Δ*pht1*Δ strain. 5FLAG-Clr4 was expressed under the control of its native promoter and terminator, and expression was confirmed by western blotting. The empty vector pREP1 was also introduced into wild-type, *clr4*Δ, and *clr4*Δ*pht1*Δ cells. Data points and error bars represent the mean±SD of three independent experiments. p-values were calculated by two-tailed Student's t-test: *p<0.05, **p<0.01, and ***p<0.001.

3-3.3 H2A.Z directly involved in RNAi-independent heterochromatin assembly.

Because *pht1*$^{+}$ regulates euchromatic genes, it is possible that loss of Pht1 reduces the expression of factors involved in RNAi-independent heterochromatin formation, resulting in the observed decrease in H3K9me in *dcr1Δ* cells. Therefore, I next measured the expression of *clr4*$^{+}$, *sir2*$^{+}$, *rrp6*$^{+}$, and *dhp1*$^{+}$, which are required for the maintenance of H3K9me in RNAi mutants (Buscaino et al., 2013; Chalamcharla et al., 2015; Ragunathan et al., 2015; Reyes-Turcu et al., 2011; Tucker et al., 2016). The expression of these genes was unaltered by the disruption of *dcr1*$^{+}$ and *pth1*$^{+}$ (Figure 14), suggesting a direct role for *pht1*$^{+}$ during H3K9me assembly.

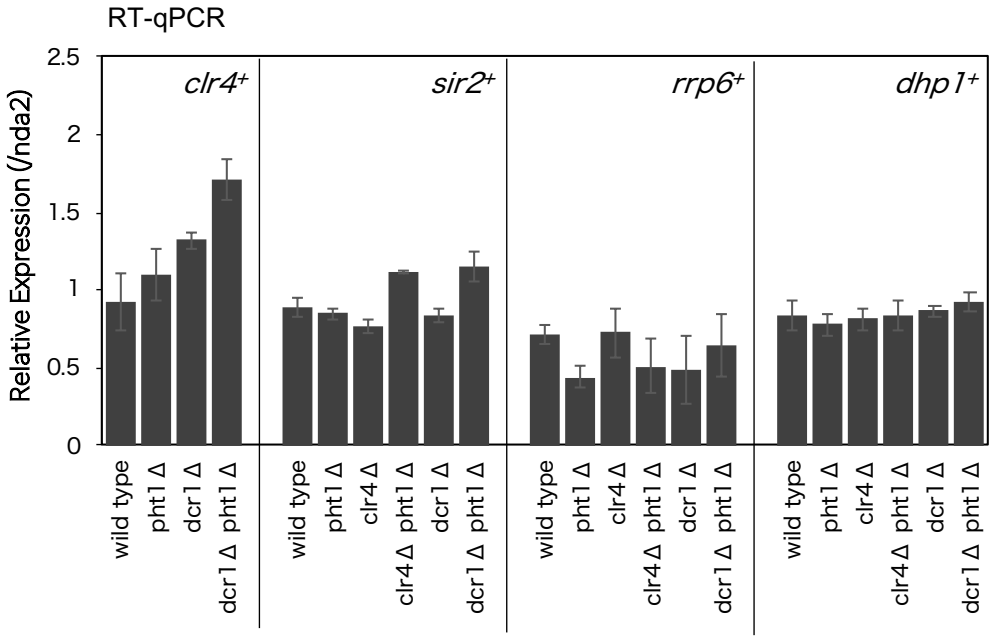

Figure 14 Deletion of Pht1 does not decrease other silencing factors. Expression of *clr4*$^{+}$, *sir2*$^{+}$, *rrp6*$^{+}$, and *dhp1*$^{+}$ was analyzed by RT-qPCR. *nda2*$^{+}$ was used as a reference gene. Data points and error bars represent the mean±SD of three independent experiments.

3-3.4 H2A.Z acts in parallel with 3'-5' exonuclease, Rrp6.

The 3'-5' exonuclease Rrp6, like Pht1, is required for RNAi-independent H3K9 methylation (Reyes-Turcu et al., 2011). Moreover, both *pht1Δ* cells and *rrp6Δ* cells have transcription termination defects in euchromatin (Zofall et al., 2009). To examine whether Pht1 and Rrp6 function together to control heterochromatic ncRNA transcription, I examined the expression of *nam7* ncRNA, which is located at pericentromeric repeats. Non-coding gene, *nam7* produces transcripts containing Mmi1 binding sequence (Touat-Todeschini et al., 2017). Since Mmi1 recruits Rrp6, which is a catalytic subunit of exosome and degrades the transcripts, *nam7* expression is suppressed by Rrp6 redundantly with Dcr1 and Clr4 (Touat-Todeschini et al., 2017). Therefore, loss of Rrp6 generates *nam7* read-thorough transcripts in *clr4*Δ cells (Touat-Todeschini et al., 2017). I found a significant accumulation of *nam7* read-through transcripts in *clr4Δrrp6Δ* cells (Figure 15A). By contrast, these transcripts did not accumulate in *clr4Δpht1Δ* cells (Figure 15A), suggesting that Pht1 does not perform the same function as Rrp6 in controlling transcription at the pericentromere. I also confirmed that loss of $pht1^{+}$ did not affect Rrp6 protein level or heterochromatic localization (Figure 15B, C). Taken together, these results suggest that Pht1 acts in parallel with Rrp6 for RNAi-independent heterochromatin assembly.

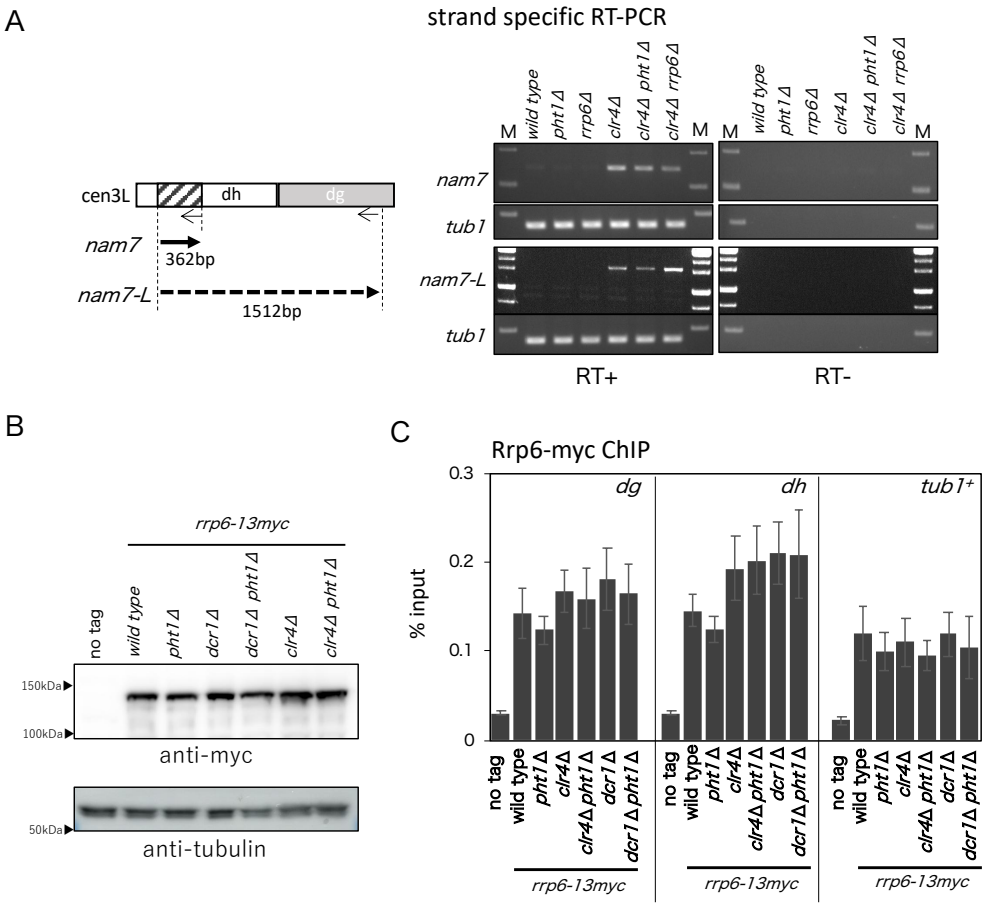

Figure 15 Deletion of *pht1*$^+$ did not affect the function or localization of Rrp6.

A) Schematic of *nam7* and *nam7* read-though transcripts (*nam7-L*). The two thin arrows represent the locations of primer used for reverse transcription. Expression of *nam7*, *nam7-L*, and *tub1*$^+$ (loading control) were analyzed by strand-specific RT-PCR. RT+ and RT- indicate the presence and absence of reverse transcriptase. M indicates the DNA ladder marker.

B) The protein levels of Rrp6-13myc and tubulin were detected by western blotting. Anti-myc antibody and anti-tubulin antibody were used.

C) The localization of Rrp6-13myc at *dg*, *dh*, and *tub1*$^+$ was analyzed by ChIP-qPCR. Data points and error bars represent the mean±SD of three independent experiments. *p*-values were calculated by two-tailed Student's *t*-test: **p*<0.05, ***p*<0.01, and ****p*<0.001.

3-3.5 H2A.Z facilitates RNAi independent heterochromatin assembly at the mat locus

I have shown that *pht1*$^{+}$ contributes to the RNAi-independent maintenance of H3K9me at pericentromeric heterochromatin and suppresses heterochromatic ncRNA transcription in the absence of H3K9me. Next, I examined whether Pht1 functions in a similar way at the *mat* locus heterochromatin, where RNAi is dispensable for heterochromatin assembly due to the presence of an Atf1/Pcr1-dependent heterochromatin assembly system (Jia et al., 2004). I first tested the silencing of a *ura4*$^{+}$ marker gene, inserted into the *mat* locus heterochromatin (*kint2::ura4*$^{+}$), by spot assay on 5-Fluoroorotic Acid (5-FOA) containing media or media lacking uracil (-URA) (Figure 16A). Since *kint2::ura4*$^{+}$ is transcriptionally silenced by heterochromatin, wild-type cells can grow on 5-FOA-containing plates but could not form colonies in the absence of uracil. By contrast, *clr4Δ* cells were sensitive to 5-FOA and could grow on -URA plates. As RNAi is not essential for heterochromatin maintenance at the *mat* locus, *dcr1Δ* cells exhibited 5-FOA resistance. Loss of *pht1*$^{+}$ did not affect silencing of *kint2::ura4*$^{+}$ in wild-type and *clr4*Δ cells. Interestingly, *dcr1Δpht1Δ* cells exhibited moderate 5-FOA sensitivity and increased growth on -URA plates compared with *dcr1Δ* cells. These results suggest that Pht1 is also required for RNAi-independent heterochromatic silencing at the *mat* locus.

To provide quantitative data for these observations, I next measured *kint2::ura4*$^{+}$ expression by RT-qPCR (Figure 16B). I also analyzed the expression of native ncRNA transcribed from *cenH,* which are highly homologous to the *dg/dh* repeats at the pericentromere (Figure 16B). Loss of *pht1*$^{+}$ did not affect *ura4*$^{+}$ expression in wild-type or *clr4Δ* cells, while *cenH* ncRNA expression increased 2.2-fold when *pht1*$^{+}$ was disrupted in a *clr4Δ* background, suggesting that the suppressive effects of Pht1 are specific for heterochromatic repeats. As previously reported (Hall et al., 2002), *kint2::ura4*$^{+}$ expression was increased 5-fold in *dcr1Δ* cells. Consistent with the spot assays in Figure 16A, *dcr1Δpht1Δ* cells exhibited 3- to 5-fold higher *ura4*$^{+}$ mRNA expression than *dcr1Δ* cells. Loss of *pht1*$^{+}$ also caused a 15- to 40-fold increase in *cenH* RNA expression in *dcr1*Δ cells, as a stimulatory effect similar to that on pericentromeric *dg*/*dh* ncRNA (Figure 10A).

I next analyzed the occupancy of transcribing RNA polymerase II by measuring Rpb1 phosphorylated at CTD Ser2 using ChIP-qPCR (Figure 16C). While loss of *pht1*$^{+}$ in wild-type cells did not affect the amount of active RNA polymerase II at either *kint2::ura4*$^{+}$ or *cenH*, loss of *pht1*$^{+}$ in *dcr1Δ* or *clr4*Δ cells led to increased occupancy of active RNA polymerase II, correlating with increased transcription. These results indicate that the accumulation of these transcripts in *pht1*Δ cells was, at least in part, a result of increased transcription. These results suggest that Pht1 is required for transcriptional gene silencing at the *mat* locus when Clr4 or Dcr1 is lost.

The data presented above suggests that loss of Pht1 might affect H3K9me levels at the *mat* locus in *dcr1Δ* cells, as observed at pericentromeric heterochromatin. To confirm this hypothesis, I performed H3K9me ChIP-qPCR (Figure 16D). As reported previously (Jia et al., 2004), H3K9me levels were maintained in *dcr1Δ* cells due to the Atf1/Pcr1-dependent heterochromatin formation system. While H3K9me at *kint2::ura4*$^{+}$ and *cenH* were unaffected by the loss of *pht1*$^{+}$ in wild-type cells, H3K9me levels decreased in *dcr1Δpht1Δ* cells at both loci (Figure 16D), suggesting that *pht1*$^{+}$ is required for efficient H3K9me maintenance in the absence of RNAi.

In addition, I note that loss of *pht1*$^{+}$ did not affect the expression of marker genes inserted into pericentromeric heterochromatin (*imr::ura4*) in *dcr1*Δ and *clr4*Δ cells (Figure 17). In *dcr1*Δ cells, H3K9me on the marker gene is abolished at pericentromeric heterochromatin but retained at the *mat* locus (Figure 16D). Thus, the different effects of Pht1 loss on expression of marker genes at these loci may reflect a difference in H3K9me occupancy. In other words, H3K9me might be required for Pht1-mediated repression in *dcr1*Δ cells.

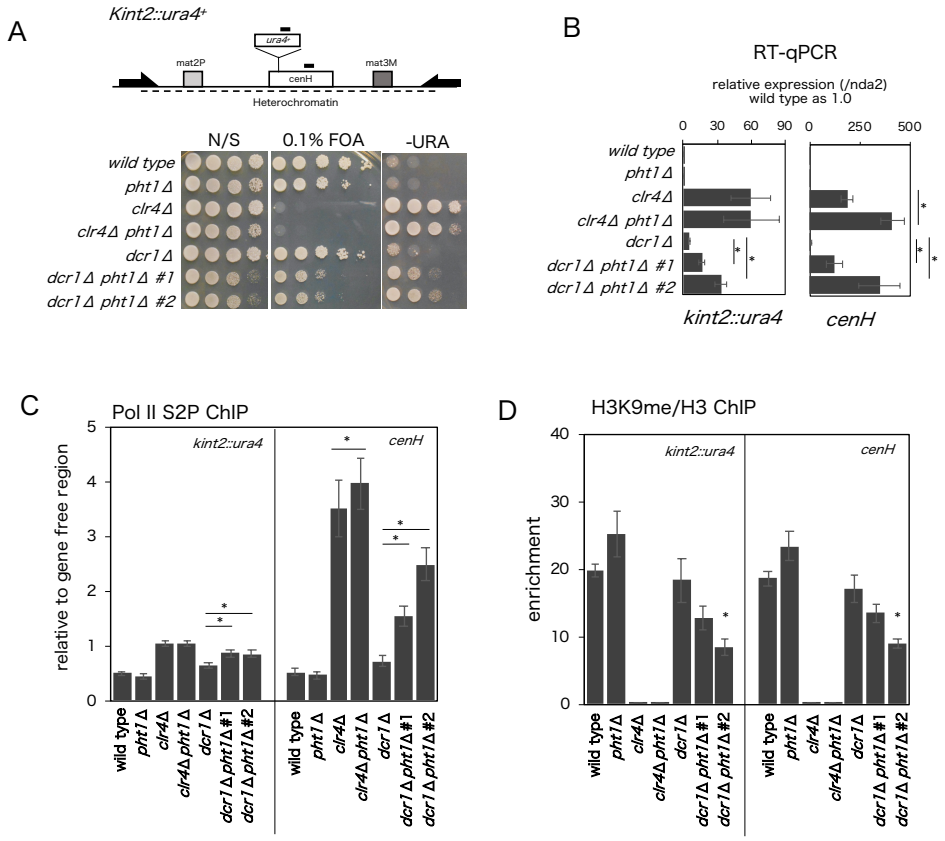

Figure 16 H2A.Z is required for RNAi-independent heterochromatin assembly at the *mat* locus.

A) Schematic of the *mat* locus in fission yeast. The *ura4*$^+$ marker gene was inserted into *cenH* (*kint2::ura4*$^+$). The two black bars indicate the location of primers used in the following experiments. *cenH* primers are located at *cenH* specific region. Ten-fold serial dilutions of the indicated strains were spotted onto YES media (N/S), 0.1% 5FOA containing media, and media lacking uracil (-URA). Plates were cultured for 3 days at 30 °C.

B) Relative expression of *kint2::ura4*$^+$ and *cenH* measured by RT-qPCR. *nda2*$^+$ was used as a control. Expression was normalized to wild type.

C) Relative enrichment of Ser2 phosphorylated RNA polymerase II at *kint2::ura4*$^+$ and *cenH* analyzed by ChIP-qPCR. Each signal was normalized to a gene free region.

D) Relative enrichment of H3K9me at *kint2::ura4*$^+$ and *cenH* analyzed by ChIP-qPCR. Each signal was normalized to H3. Data points and error bars in B–D represent the mean±SD of three independent experiments. *p*-values were calculated by two-tailed Student's *t*-test: **p*<0.05, ***p*<0.01, and ****p*<0.001.

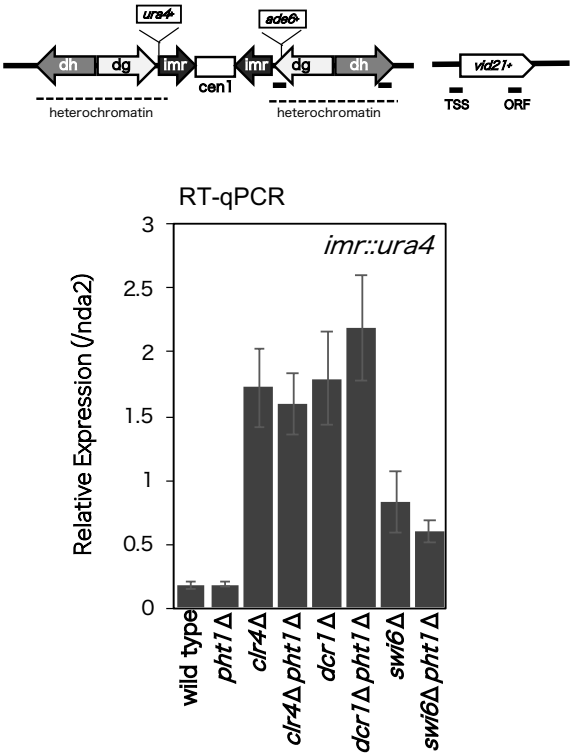

Figure 17 Loss of Pht1 did not affect *imr::ura4* expression.
Expression of *imr::ura4*$^{+}$ was analyzed by RT-qPCR. *nda2*$^{+}$ was used as a reference gene. Data points and error bars represent the mean±SD of three independent experiments. *p*-values were calculated by two-tailed Student's *t*-test: **p*<0.05, ***p*<0.01, and ****p*<0.001.

3-3.6 H2A.Z is required for sub-telomeric gene silencing.

Loss of Pht1 has been reported to be involved in the silencing of sub-telomeric genes without affecting H3K9 methylation (Zofall et al., 2009). However, the mechanism for this remains unclear. Therefore, I next investigated Pht1 function in the sub-telomeric region. I first measured the expression of the subtelomeric genes *tlh1*$^{+}$ and *tlh2*$^{+}$ (Figure 18A). *tlh1*$^{+}$ and *tlh2*$^{+}$ is located at chromosome I and II, respectively. It is worth noting that the primers represent +1 nucleosome, where homologous region of *tlh1*$^{+}$ and *tlh2*$^{+}$, thus I could not distinguish between *tlh1*$^{+}$ and *tlh2*$^{+}$. Since *tlh1/2*$^{+}$ contain sequences homologous to pericentromeric repeats, RNAi is able to act upon these genes (Kanoh et al., 2005). However, it has been shown that RNAi mutants do not significantly affect silencing because the telomeric DNA-binding protein Taz1 protein recruits Clr4 to the telomeric region, and H3K9me is maintained by Clr4 self-propagation (Wang et al., 2016). On the other hand, loss of Swi6 significantly decreases telomeric silencing (Kanoh et al., 2005). In *pht1Δ* cells, *tlh1/2*$^{+}$ mRNA levels were increased nearly 10-fold as reported before (Zofall et al., 2009). Although *dcr1*$^{+}$ disruption did not affect *tlh1/2*$^{+}$ expression, additive silencing defects were observed in *dcr1Δpht1Δ* cells. A similar defect was seen in *clr4Δpht1Δ* cells. While *swi6*Δ cells increased *tlh1/2*$^{+}$ expression, *swi6*Δ*pht1*Δ did not. I next measured RNA Pol II occupancy in these cells (Figure 18B). While no difference in Pol II occupancy was observed in *dcr1Δ* cells, occupancy rose 1.7-fold in *pht1Δ* cells and 3.2-fold in *dcr1Δpht1Δ* cells. A slight increase in Pol II occupancy was observed in *clr4Δpht1Δ* cells compared with *clr4Δ* cells, while *swi6*Δ as well as *swi6*Δ*pht1*Δ cells exhibited same occupancy. These data suggest that Pht1 participates in transcriptional gene silencing at sub-telomeric heterochromatin in both wild-type cells and *dcr1Δ*/*clr4Δ* cells but not *swi6*Δ cells.

Next, I asked whether Pht1 affects H3K9 methylation at subtelomeres (Figure 18C). While *pht1*$^{+}$ disruption caused silencing defects, the level of H3K9me was slightly increased. H3K9me was retained in *dcr1Δ* cells at a similar level to the wild type, but decreased in *dcr1Δpht1Δ* cells. While *swi6*Δ cells decreased H3K9me, loss of Pht1 did not affect H3K9me in *swi6*Δ cells. These results indicate that Pht1 plays a critical role in telomeric gene silencing and is required for efficient RNAi-independent H3K9me maintenance.

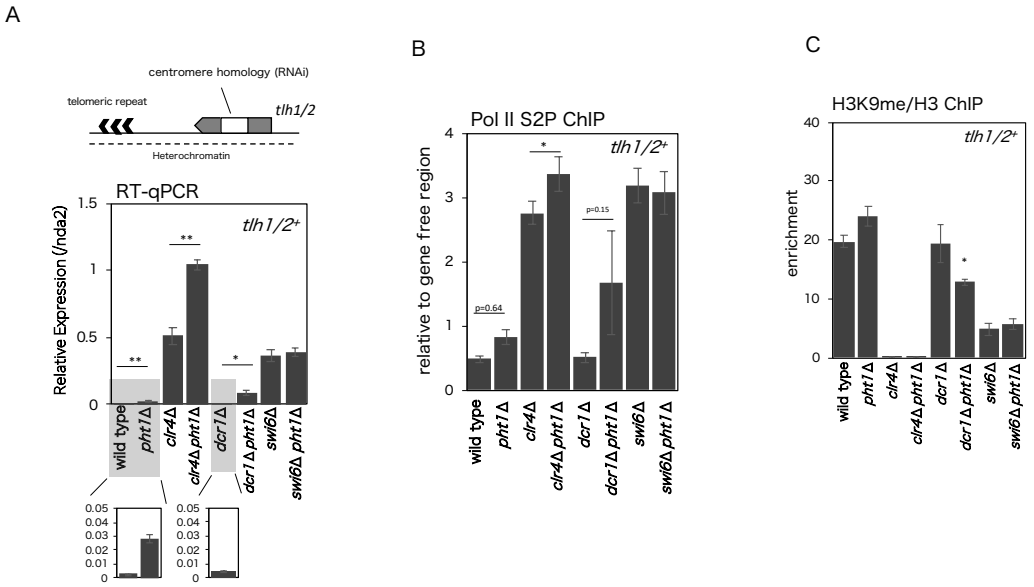

Figure 18 H2A.Z is required for subtelomeric silencing.

A) Relative expression of *tlh1/2*$^+$ was measured by RT-qPCR. Primers are located at the homologous region of *tlh1*$^+$ and *tlh2*$^+$, which represent +1 nucleosome. *nda2*$^+$ was used as a reference gene.

B) Relative enrichment of Ser2 phosphorylated RNA polymerase II at *tlh1/2*$^+$ was analyzed by ChIP-qPCR. Each signal was normalized to a gene free region.

C) Relative enrichment of H3K9me at *tlh1/2*$^+$ was analyzed by ChIP-qPCR. Each signal was normalized to H3. Data points and error bars represent the mean±SD of three independent experiments. *p*-values were calculated by two-tailed Student's *t*-test: **p*<0.05, ***p*<0.01, and ****p*<0.001.

3-4 H2A.Z facilitates RNAi-independent heterochromatin assembly by antagonizing Epe1-mediated demethylation.

3-4.1 H2A.Z is not directly involved in RNAi-independent heterochromatin assembly.

I have shown that *pht1*$^{+}$ is required for RNAi-independent maintenance of H3K9me at all heterochromatin loci. H3K9me can be maintained by Clr4 self-propagation via the chromodomain of Clr4 in the absence of RNAi (Ragunathan et al., 2015). Thus, I tested whether Pht1 is involved in Clr4-mediated self-propagation of H3K9me using an artificial heterochromatin formation system and a TetR-Clr4 fusion protein. In this system, TetR fused Clr4 binds to a *tetO::ade6*$^{+}$ locus and establishes ectopic heterochromatin in the absence of anhydrotetracycline (-AHT), resulting in the red colony formation on low adenine media (Audergon et al., 2015; Ragunathan et al., 2015). Addition of AHT releases TetR::Clr4 from *tetO::ade6*$^{+}$. Epe1, which functions as an eraser of H3K9me, removes H3K9me and the colonies become white. However, in *epe1*Δ cells, H3K9me is maintained through Clr4-mediated self-propagation and some cells keep their red color (Audergon et al., 2015). Therefore, to assess contribution of Pht1, I examined whether loss of *pht1*$^{+}$ affected the maintenance of ectopic heterochromatin at *tetO::ade6*$^{+}$. In the absence of AHT, both wild-type and *pht1*Δ cells formed red colonies (Figure 19), indicating that Pht1 is not involved in the establishment of heterochromatin by TetR-Clr4. When these red colonies were transferred to media containing AHT, both wild-type and *pht1*Δ colonies became white. Furthermore, *epe1*Δ and *epe1*Δ *pht1*Δ cells exhibited a red colony phenotype, suggesting that *pht1*$^{+}$ is not required for the maintenance of ectopic heterochromatin in *epe1*Δ cells (Figure 19). These results indicate that *pht1*$^{+}$ is not directly involved in Clr4-mediated self-propagation of heterochromatin.

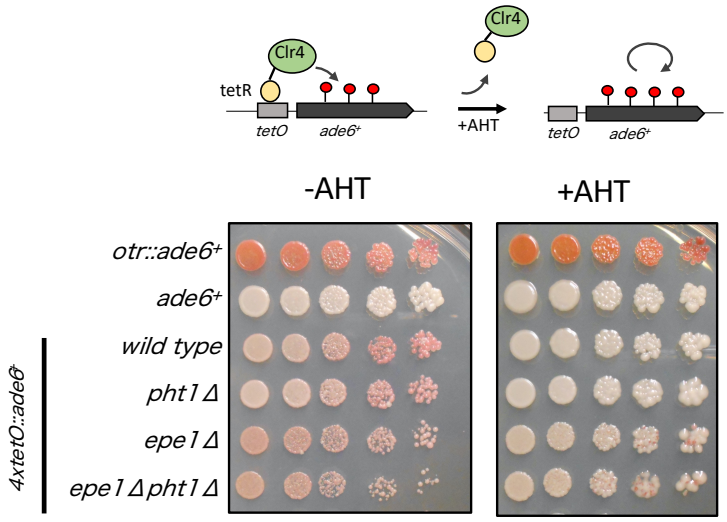

Figure 19 H2A.Z was not required for TetR-Clr4 mediated heterochromatin assembly.

Schematic of establishment and maintenance of heterochromatin at *4xtetO::ade6*$^{+}$. TetR-Clr4 were released by the addition of anhydrotetracycline (AHT) and repressed by the addition of thiamine. Five-fold dilutions of the indicated strains were spotted onto PMG low ade media (containing 7.5 mg/L adenine) with or without 10 µM AHT and 5 mg/L thiamin (+AHT or -AHT, respectively). Plates were incubated for 5 days at 30 °C. *otr::ade6*$^{+}$ and *ade6*$^{+}$ strains were used as controls for red and white colony formation, respectively.

3-4.2 H2A.Z inhibits Epe1-mediated H3K9 demethylation, which is required for H3K9me maintenance.

As mentioned above, Epe1 erases H3K9me, and the maintenance of H3K9me relies on a balance between "writer" and "eraser". For example, while RNAi mutants show silencing defects caused by a decrease in H3K9me, loss of *epe1*$^{+}$ in RNAi deficient cells restores H3K9 methylation and silencing, indicating that H3K9me at pericentromere could be maintained without RNAi in the absence of "eraser" (Trewick et al., 2007; Zofall and Grewal, 2006). Since Pht1 did not directly enhance Clr4 self-propagation (Figure 19), I wondered whether Pht1 maintains H3K9me in the absence of RNAi by repressing Epe1-dependent H3K9 demethylation. To elucidate this, I made *epe1Δdcr1Δpht1Δ* triplet mutants. Since loss of *epe1*$^{+}$ bypasses silencing defects in RNAi deficient cells, *epe1*Δ*ago1*Δ cells generate a variegated phenotype on low adenine plates, which is identical to *epe1*Δ phenotype (Sorida et al., 2019). In this study, I found that *epe1*Δ*dcr1*Δ cells also exhibited this variegated phenotype (Figure 20) and became 5FOA resistant, indicating that loss of *epe1*$^{+}$ suppresses the silencing defects of *dcr1*Δ. *epe1Δdcr1Δpht1Δ* cells also generated variegated colonies, suggesting that *otr*::*ade6* is still silent in some colonies (Figure 20). For further investigation, I obtained two clones: a 5FOA sensitive (#1) and a 5FOA resistant clone (#2) (Figure 20). While *epe1*Δ*dcr1*Δ*pht1*Δ cells still showed variegated phenotype like *epe1*Δ cells, *epe1*Δ*dcr1*Δ*pht1*Δ*#2* cells exhibited more silent red colonies than *epe1*Δ*dcr1*Δ*pht1*Δ*#1* cells, which was in agreement with 5FOA sensitivity (Figure 20).

I measured H3K9me levels in these clones by ChIP-qPCR (Figure 21). As previously observed, I found that *epe1*Δ*dcr1*Δ double deletion restored H3K9me at *dg/dh* to an almost wild-type level. H3K9me at *imr::ura4*$^{+}$ was completely lost in *dcr1*Δ cells but partially restored by further disruption of *epe1*$^{+}$. Consistent with the spot assays, H3K9me at *imr::ura4*$^{+}$ was completely abolished in *epe1*Δ*dcr1*Δ*pht1*Δ*#1* clone but was restored in clone *epe1*Δ*dcr1*Δ*pht1*Δ*#2*. H3K9me at *dg/dh* regions was increased 5-fold in *epe1*Δ*dcr1*Δ*pht1*Δ*#1* compared with *dcr1*Δ*pht1*Δ cells, while H3K9me loading was fully restored in *epe1*Δ*dcr1*Δ*pht1*Δ*#2* cells. Although levels of H3K9me were variable, *epe1*Δ*dcr1*Δ*pht1*Δ cells restored H3K9me at *dg/dh*, suggesting that *epe1*$^{+}$ is responsible for the depletion of H3K9me in *dcr1*Δ*pht1*Δ cells. Although it was still possible that Pht1 regulates *epe1*

expression level and affects H3K9me, loss of *dcr1*$^{+}$ and/or *pht1*$^{+}$ did not affect *epe1*$^{+}$ mRNA levels (Figure 22). Therefore, these results suggest that loss of Pht1 directly enhances the function of *epe1*$^{+}$ as an eraser of H3K9me. Taken together, Pht1 facilitates RNAi-independent heterochromatin assembly by suppressing Epe1-mediated demethylation.

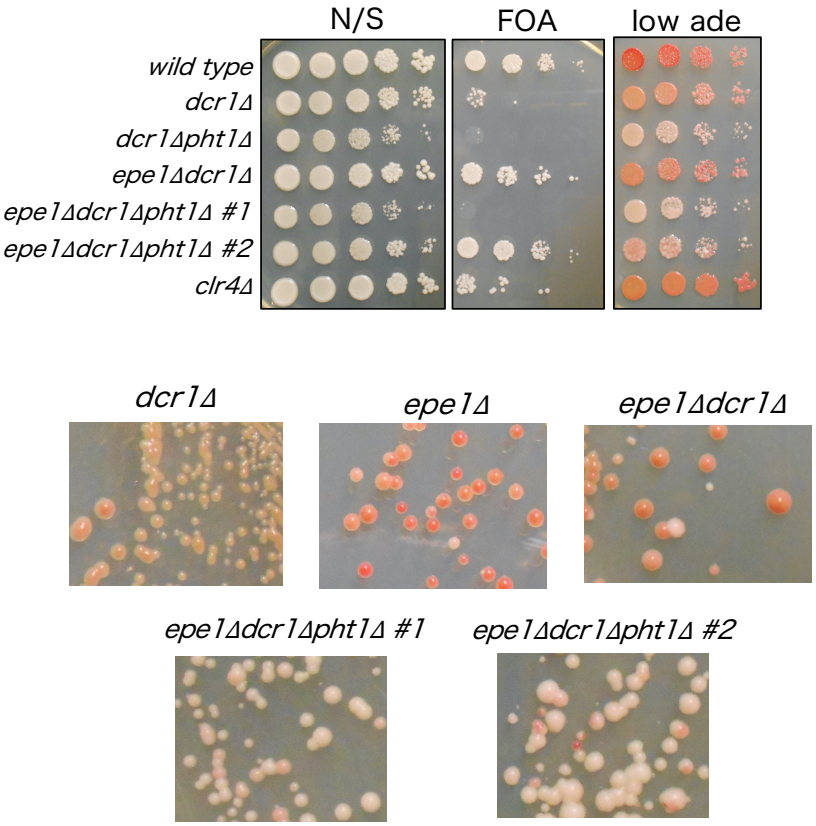

Figure 20 variegated phenotypes of epe1Δdcr1Δpht1Δ cells.
Five-fold dilutions of the indicated strains were spotted onto YES media, 5FOA containing media, and YES media without adenine (low ade). Plates were cultured for 3 days at 30 °C. To clearly see the variegated phenotype, *dcr1*Δ, *epe1*Δ, *epe1*Δ*dcr1*Δ, *epe1*Δ*dcr1*Δ*pht1*Δ *#1*, and *epe1*Δ*dcr1*Δ*pht1*Δ *#2* strains were streaked on low ade plates (lower panels).

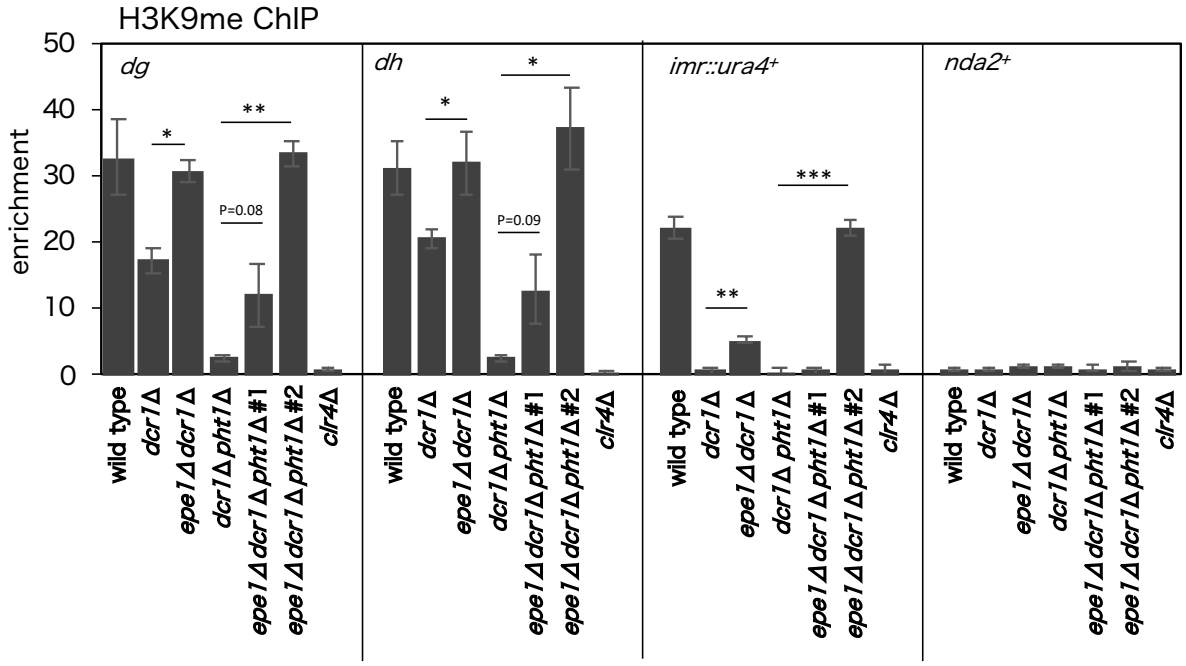

Figure 21 *epe1*Δ*dcr1*Δ*pht1*Δ cells restore H3K9me at pericentromere.

Localization of H3K9me at *dg*, *dh*, *imr*::*ura4*$^+$, and *nda2*$^+$ was analyzed by ChIP-qPCR. *nda2*$^+$ was used as a negative control. Data points and error bars represent the mean±SD of three independent experiments. *p*-values were calculated by two-tailed Student's *t*-test: **p*<0.05, ***p*<0.01, and ****p*<0.001.

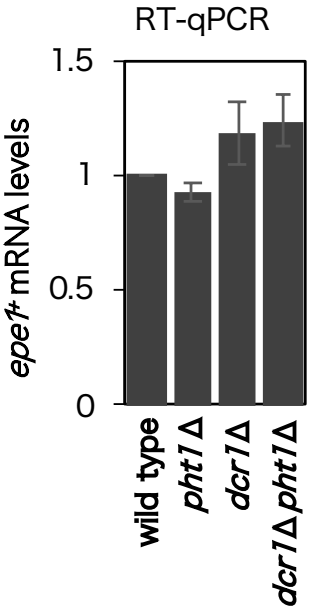

Figure 22 loss of *dcr1*$^+$ and/or *pht1*$^+$ does not affect *epe1*$^+$ mRNA level. Expression of *epe1*$^+$ relative to *nda2*$^+$ measured by RT-qPCR. Data points and error bars represent the mean±SD of three independent experiments.

3-5 H2A.Z facilitates subtelomeric gene repression by inhibiting Epe1-mediated transcription.

3-5.1 H2A.Z inhibits transcription activation of Epe1.

Epe1 has a transcription activation domain at its N-terminus to prevent ectopic heterochromatin formation (Sorida et al., 2019), and overexpression of Epe1 increases transcription at heterochromatic regions (Aygun et al., 2013; Trewick et al., 2007). Thus, I considered whether loss of *pht1*$^{+}$ could also enhance transcription activation by Epe1. To analyze this, I overexpressed Epe1 from a *urg1*$^{+}$ promoter (*epe1OP*) and measured *dg/dh* expression by RT-qPCR (Figure 23A). *epe1OP pht1*Δ cells exhibited an epistatic increase in ncRNA expression. Using ChIP-qPCR, I found that Ser2 phosphorylated RNA Pol II loading was also synergistically increased in these cells (Figure 23B). Because it was still possible that this synergistic increase of Pol II occupancy is caused by the decrease of H3K9me, I measured H3K9me levels in these cells. However, the levels of H3K9me did not change (Figure 23C), suggesting that loss of H3K9 methylation was not the cause of this synergistic increase in transcription. Taken together, these results show that Pht1 represses transcription activation by *epe1*$^{+}$.

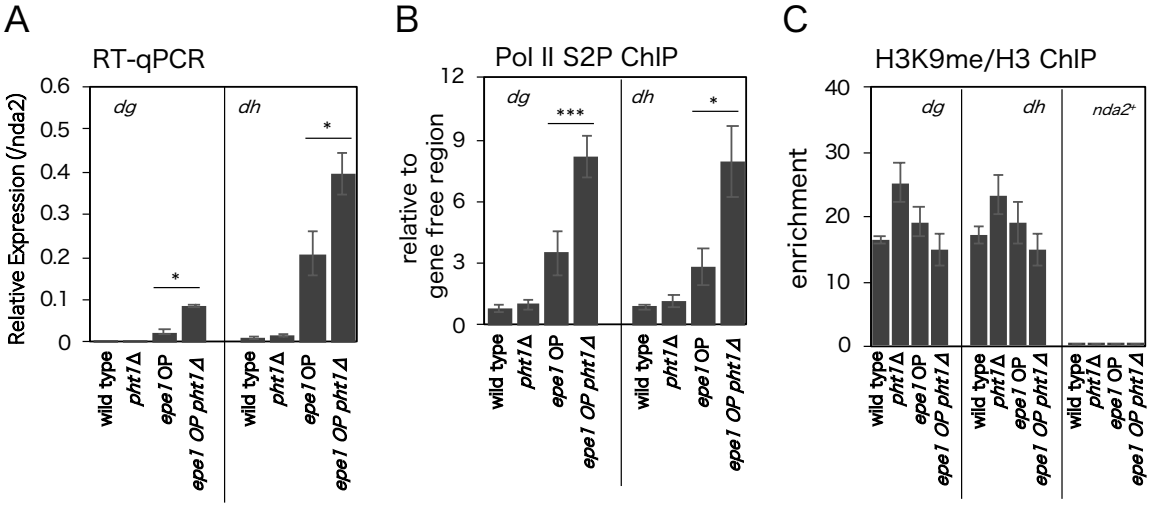

Figure 23 H2A.Z antagonizes Epe1-mediated transcription.

A) Expression of dg and dh relative to *nda2*$^{+}$ was measured by RT-qPCR.

B) Relative enrichment of Ser2 phosphorylated RNA polymerase II at *dg* and *dh* was analyzed by ChIP-qPCR. Each signal was normalized to a gene free region.

C) Relative enrichment of H3K9me at *dg* and *dh* was analyzed by ChIP-qPCR. Each signal was normalized to H3. *nda2*$^{+}$ was used as a negative control. Data points and error bars represent the mean±SD of three independent experiments. *p*-values were calculated by two-tailed Student's *t*-test: **p*<0.05, ***p*<0.01, and ****p*<0.001

3-5.2 Epe1 is responsible for the derepression of subtelomeric gene in *pht1*Δ cells.

At subtelomeric heterochromatin (*thl1/2*), loss of Pht1 caused transcriptional activation (Figure 18). Thus, I wondered whether *epe1*$^+$ is required for transcriptional activation in *pht1*Δ cells. If this were the case, loss of *epe1*$^+$ would suppress *tlh1/2*$^+$ expression in *pht1*Δ cells. To elucidate this, I measured *tlh1/2*$^+$ expression by RT-qPCR in various *epe1*$^+$ and *pht1*$^+$ disruption mutants (Figure 24A). *epe1*Δ*pht1*Δ cells showed decreased *tlh1/2*$^+$ expression compared with *pht1*Δ cells, suggesting that Epe1 is responsible for transcriptional activation at subtelomeric heterochromatin in the absence of *pht1*$^+$. Furthermore, I confirmed that H3K9me levels did not change in *epe1*Δ*pht1*Δ cells, indicating that changes in *tlh1/2*$^+$ expression were not due to changes in the level of H3K9me (Figure 24B). Furthermore, disruption of *pht1*$^+$ did not alter the localization of 3Flag-Epe1 at the *tlh1/2*$^+$ locus, suggesting that Pht1 suppressed the function of Epe1 (Figure 24C). In conclusion, Pht1 is required for subtelomeric gene silencing by repressing Epe1-mediated transcription.

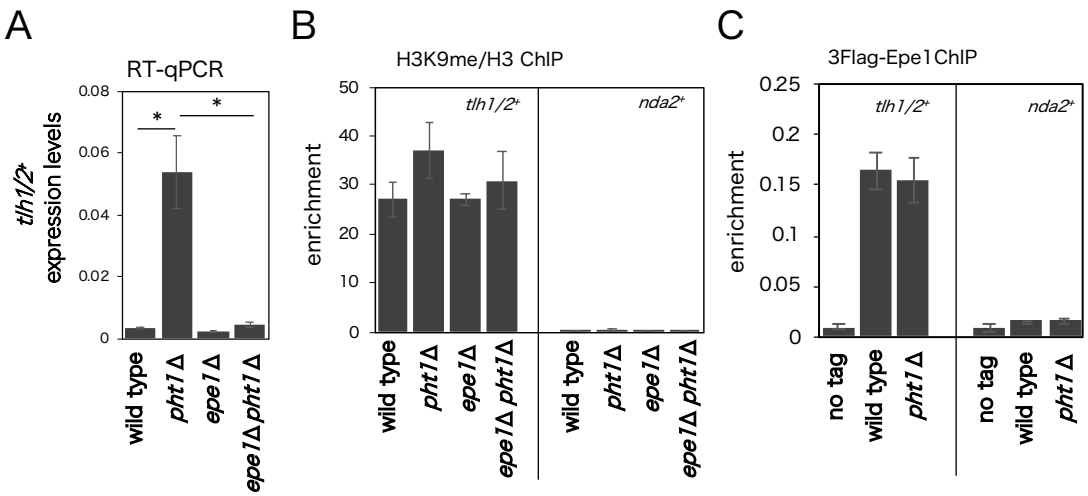

Figure 24 loss of Epe1 restored the derepression of subtelomeric gene in *pht1*Δ cells.

A) Expression of *tlh1/2*$^+$ relative to *nda2*$^+$ measured by RT-qPCR.

B) Relative enrichment of H3K9me at *tlh1/2*$^+$ and *nda2*$^+$ analyzed by ChIP-qPCR. Each signal was normalized to H3.

C) Localization of 3FLAG-Epe1 at *tlh1/2* and *nda2*$^+$ was measured by ChIP-qPCR. Data points and error bars in B–H represent the mean±SD of three independent experiments. *p*-values were calculated by two-tailed Student's *t*-test: **p*<0.05, ***p*<0.01, and ****p*<0.001. Data points in C represent the average of % input from two independent experiments. Error bars represent ±SD.

3-6 The N-terminal region of Pht1 is required for transcriptional repression in *clr4*Δ cells.

3-6.1 H2A.Z represses pericentromeric ncRNA in *clr4*Δ cells independently of H3K14ac and H3K4me.

I have shown that Pht1 maintains gene silencing by repressing Epe1-dependent H3K9me removal in *dcr1*Δ cells. However, this silencing mechanism is not applicable in *clr4Δ* cells because the localization of Epe1 depends on H3K9me (Zofall and Grewal, 2006). To understand this mechanism, I next measured two euchromatic markers: H3K14 acetylation and H3K4 methylation (Figure 25A, B). Loss of Clr4 increased both H3K14ac and H3K4me3 as observed previously (Noma et al., 2001; Yamada et al., 2005). However, no cumulative increase in these active modifications was seen in *clr4Δpht1Δ* cells, suggesting that Pht1-dependent repression of transcription in *clr4Δ* was independent of H3K14ac and H3K4me3.

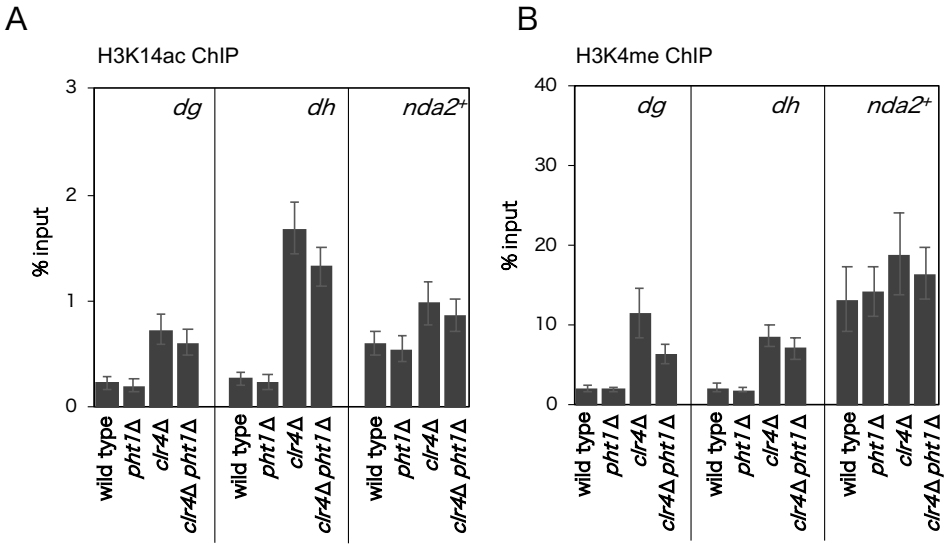

Figure 25 H2A.Z suppresses transcription without affecting H3K14ac and H3K4me3.

A–B) Localization of H3K14ac (A) and H3K4me3 (B) at *dh*, dh, and *nda2*$^{+}$ was analyzed by ChIP-qPCR. Data points and error bars represent the mean±SD of three independent experiments. *p*-values were calculated by two-tailed Student's *t*-test: **p*<0.05, ***p*<0.01, and ****p*<0.001.

3-6.2 N-terminus of H2A.Z is essential for transcriptional repression in *clr4*Δ cells.

Acetylation of the N-terminal lysine of H2A.Z is a well conserved modification (Giaimo et al., 2019). In fission yeast, N-terminal mutations can both positively and negatively affect the expression of various genes (Kim et al., 2009). Thus, I speculated that the Pht1 N-terminus is required for the repression of pericentromeric ncRNA in *clr4*Δ cells. To investigate this, we introduced three different mutations into the Pht1 N-terminus in a wild-type and *clr4Δ* background: deletion of N-terminal residues (ΔN), acetylation mimetic mutant (4KQ), and an acetylation negative mutant (4KR) (Figure 26A). Western blot shows that the protein levels of these myc-tagged Pht1 mutants were equivalent (Figure 26B). Moreover, we found that these mutations did not affect localization to *vid21*$^{+}$ TSS and ORF (Figure 26C). As with wild-type Pht1, the localization of Pht1ΔN, Pht1(4KQ), and Pht1(4KR) at *dh* was increased in a *clr4Δ* background (Figure 26C), demonstrating that these N-terminal mutations did not affect the regulation of Pht1 localization at defective heterochromatin. This is consistent with the previous observation that Swr1 recognizes C-terminal helix of H2A.Z (Hong et al., 2014). Next, I analyzed the effect that these Pht1 N-terminal mutants had on the expression of *dh* ncRNA (Figure 26D). While these mutants did not affect *dh* ncRNA expression in a wild-type background, *pht1ΔN*, *pht1(4KQ)*, and *pht1(4KR)* increased *dh* expression in *clr4Δ* cells, though the extent of the increase was smaller than in *clr4*Δ*pht1*Δ cells. These results suggest that the N-terminal region of Pht1 is required for H3K9me independent silencing, at least in part. Interestingly, similar silencing defects were observed in both *clr4Δpht1(4KQ)* and *clr4Δpht1(4KR)* cells, suggesting that the change in charge that occurs upon acetylation is not crucial for its function. Because, in mammal, methylation at N-terminus of H2A.Z are reported (Binda et al., 2013), other modifications on N-terminus of Pht1 may exist. Although precise effects of N-terminal mutations are unclear, at least, similar expression pattern in *pht1(4KQ)* and *pht1(4KR)* cells were observed in euchromatic gene expression pattern (Kim et al., 2009), suggesting that mechanisms for ncRNA repression in *clr4*Δ cells might be identical to euchromatic gene regulation. Taken together, these data show that the N-terminus of Pht1 is required for Pht1-medated silencing of heterochromatic ncRNA at pericentromeres in the absence of H3K9me.

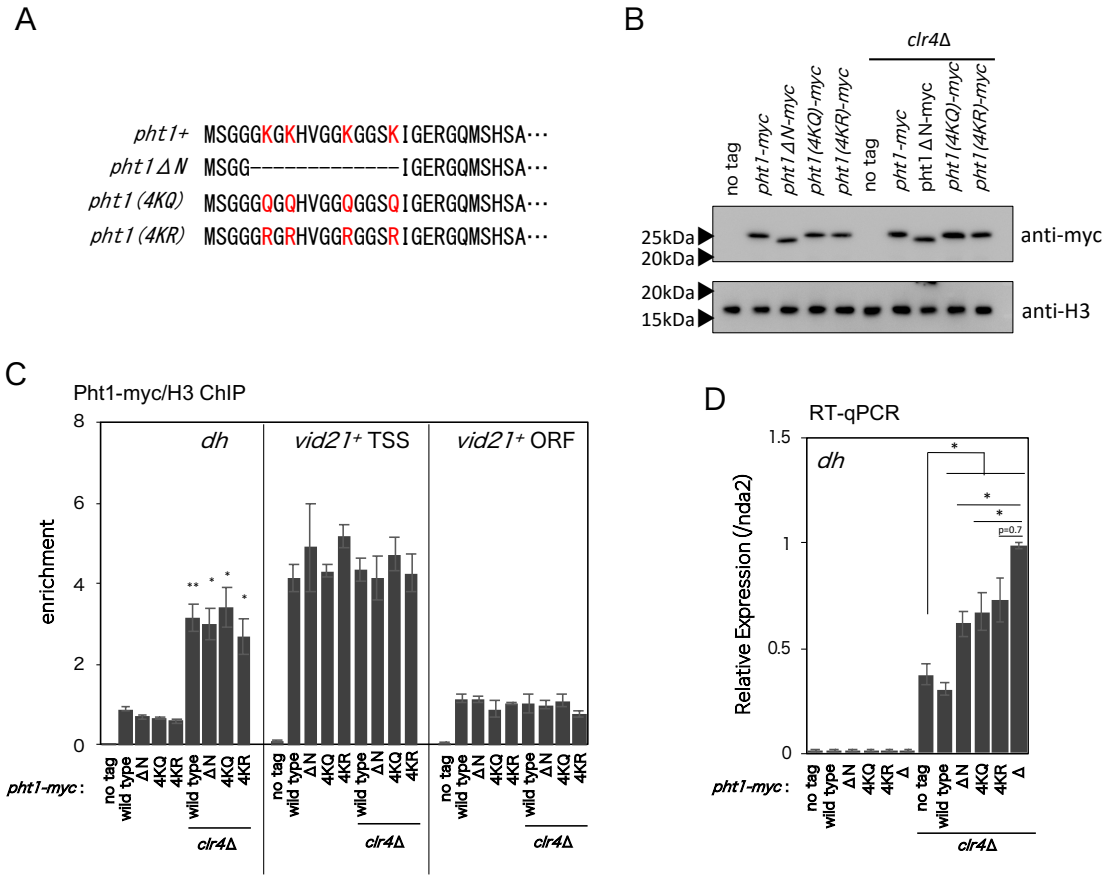

Figure 26 N-terminal region of H2A.Z is required for transcriptional repression in *clr4*Δ.

A) N terminal amino acids of *pht1*$^{+}$, *pht1ΔN*, *pht1(4KQ)*, and *pht1(4KR)* are shown.

B) Protein levels of Pht1-myc and H3 were analyzed by western blotting. Anti-myc antibody and anti-H3 antibody were used.

C) Localization of Pht1-myc analyzed by ChIP-qPCR. Signals were normalized to H3.

D) Relative expression levels of *dh* were measured by RT-qPCR. *nda2*$^{+}$ was used as a reference gene. Data points and error bars in C–D represent the mean±SD of three independent experiments. *p*-values were calculated by two-tailed Student's *t*-test: **p*<0.05, ***p*<0.01, and ****p*<0.001.

3-6.3 N-terminus of Pht1 is not involved in RNAi-independent heterochromatin assembly and subtelomeric gene repression.

I hypothesized that the silencing mechanisms of Pht1 in *clr4*Δ and *dcr1*Δ cells are different. To confirm this, I measured the effect the N-terminus of Pht1 had on heterochromatin assembly in *dcr1*Δ cells and transcriptional repression of *tlh1/2*$^{+}$. *pht1*Δ*N* did not affect H3K9me at pericentormeres in *dcr1*Δ cells (Figure 27). Furthermore, *pht1ΔN*, *pht1(4KQ)*, and *pht1(4KR)* did not exhibit de-repression activity at the *tlh1/2*$^{+}$ loci (Figure 28). These results show that the N-terminus of Pht1 is not required for the suppression of Epe1-mediated demethylation and transcription activation.

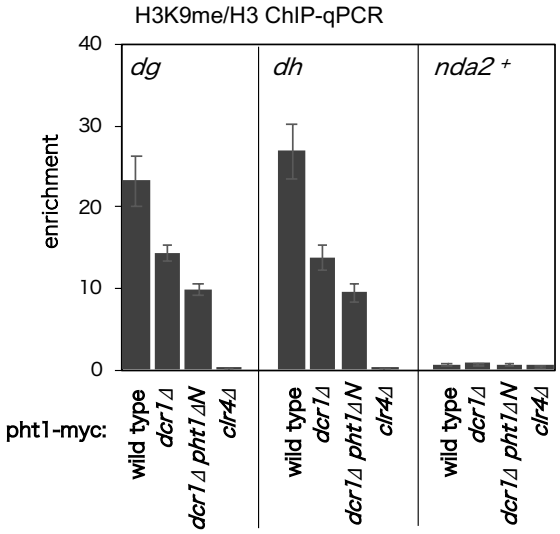

Figure 27 The N-terminus of Pht1 is not required for Epe1-mediated demethylation.

A) Localization of H3K9me at *dg*, *dh*, and *nda2*$^{+}$ was analyzed by ChIP-qPCR. Each signal was normalized to H3. *nda2*$^{+}$ is used as a negative control. Data points and error bars represent the mean±SD of two independent experiments. *p*-values were calculated by two-tailed Student's *t*-test: **p*<0.05, ***p*<0.01, and ****p*<0.001.

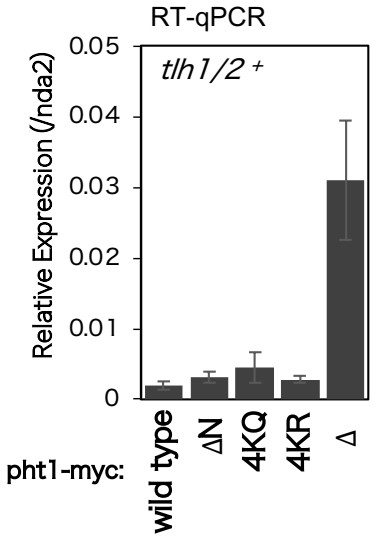

Figure 28 The N-terminus of Pht1 is not required for Epe1-mediated transcription activation.

Expression of *tlh1/2*$^{+}$ in Pht1 N-terminal mutants was analyzed by RT-qPCR. *nda2*$^{+}$ was used as a reference gene. Data points and error bars represent the mean±SD of three independent experiments. *p*-values were calculated by two-tailed Student's *t*-test: **p*<0.05, ***p*<0.01, and ****p*<0.001.

4. Discussion

As well as histone modifications, histone variants are important for the diverse nature of the chromatin functions. Several amino acids are distinct in histone variants, and while canonical histones are only synthesized during S phase, histone variants are expressed throughout the cell cycle, resulting in specific functions in many biological processes (Martire and Banaszynski, 2020). For example, H3 variant, CENPA has a specific function in kinetochore formation (De Rop et al., 2012), and H2A variant, H2A.X is required for DNA damage responses (Bönisch and Hake, 2012). Histone variant H2A.Z is one of the most evolutionally conserved histone variants and plays important roles. While its role in euchromatic gene regulation is well studied, functions in heterochromatin are poorly understood. In this study, I have shown that H2A.Z plays multiple roles at heterochromatic regions, as summarized in Figure 29. In wild-type cells, a low level of H2A.Z occupies at heterochromatic regions, which represses Epe1-dependent transcription at subtelomeric heterochromatin and represses transcription induced by Epe1-overexpression at pericentromeric heterochromatin (Figure 29A). When RNAi-dependent heterochromatin formation is lost, H2A.Z is incorporated into pericentromeric heterochromatin and facilitates RNAi-independent heterochromatin assembly not by direct involvement in Clr4 self-assembly but by repressing Epe1-dependent demethylation. H2A.Z is also required for efficient RNAi-independent heterochromatin assembly at *mat* locus and subtelomere (Figure 29B). When H3K9me is completely abolished by the loss of Clr4, H2A.Z is incorporated into heterochromatin in a SWR complex-dependent manner and represses Pol II-dependent transcription at pericentromeric repeats (Figure 29C). Taken together, these findings provide new aspects of H2A.Z in the maintenance of heterochromatin integrity.

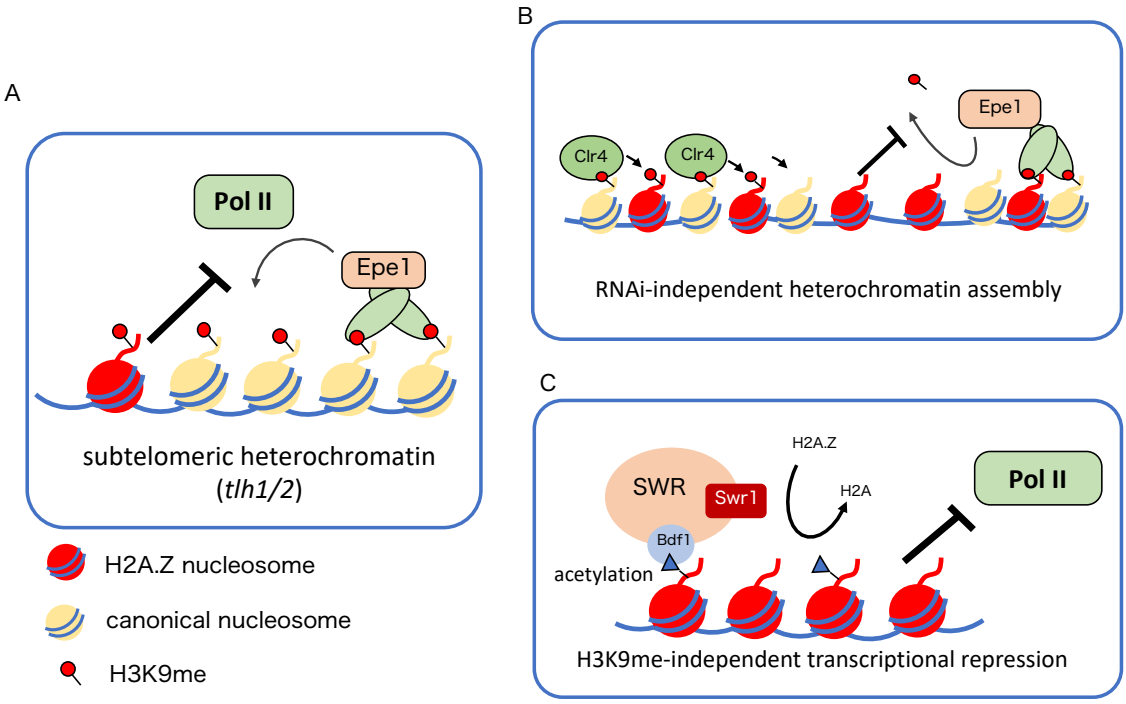

Figure 29 The roles of H2A.Z for the maintenance of heterochromatic integrity.

A) In wild-type cells, H2A.Z is poorly enriched at heterochromatin. H2A.Z suppresses Epe1-mediated transcription at subtelomere and also inhibits transcription induced by Epe1-overexpression.

B) In RNAi-deficient cells, H2A.Z accumulates at pericentromeres and is required for the maintenance of H3K9me. As H2A.Z was not directly involved in Clr4 self-assembly, H2A.Z facilitates RNAi-independent H3K9me by suppressing Epe1-mediated demethylation.

C) In *clr4*Δ cells, the SWR complex promotes H2A.Z accumulation at pericentromeres. This accumulating H2A.Z suppresses Pol II dependent-ncRNA transcription in *clr4*Δ cells but not *ura4*$^{+}$ marker gene expression inserted at heterochromatic region. The N-terminus of H2A.Z is required for this suppression.

4-1 Mechanisms for the deposition of H2A.Z at heterochromatic regions.

The negative correlation between H2A.Z and H3K9me/DNA methylation is a conserved feature of H2A.Z in higher eukaryotes (Boyarchuk et al., 2014; Zilberman et al., 2008). However, how loss of H3K9me induced H2A.Z deposition was unclear. I find that this negative correlation is also conserved in fission yeast and have shown that loss of H3K9me induced Swr1-mediated H2A.Z deposition at pericentromeric heterochromatic regions (Figure 8). Also, I show that a component of the SWR complex, Bdf1, is required for this accumulation (Figure 9B). Since Bdf1 recognizes acetylated histone tail, Bdf1 would recognize the increased level of histone acetylation associated with the loss of heterochromatin and mediates H2A.Z deposition. This could explain why H2A.Z occupancy at *dg* and *dh* are different; H3K14ac level at *dh* in *clr4*Δ cells are higher that *dg* (Figure 9A). Since high level of histone acetylations reflects TSS sites of euchromatic gene (Pokholok et al., 2005), the differences observed in *dg* and *dh* might be caused by the relative positions of primers to potential TSS in heterochromatic region. Interestingly, as previously observed in budding yeast, loss of Bdf1 does not affect H2A.Z localization at TSS of euchromatic gene because Bdf2, which is not a component of SWR complex, alternatively functions (Raisner et al., 2005). In fission yeast, Bdf1 is not required for H2A.Z enrichment at TSS of *vid21*$^{+}$ suggesting that Bdf2 contributes for SWR complex recruitment instead of Bdf1. Moreover, since Swc2 recognizes nucleosome free DNA at TSS (Ranjan et al., 2013; Yen et al., 2013), it is also possible that Swc2 alternatively recruits SWR complex to TSS of *vid21*$^{+}$ in the absence of Bdf1.

In contrast to the accumulation of H2A.Z seen at compromised heterochromatin, low levels of H2A.Z are maintained at wild-type heterochromatin by a Swr1-independent pathway. I show that H2A.Z at wild-type heterochromatin suppresses Epe1-dependent transcriptional activation (Figure 23), which suggests that the low level of H2A.Z at heterochromatin has a functional role. Actually, H2A.Z is randomly deposited at gene body (Hardy et al., 2009). One possible mechanism of Swr1-independent H2A.Z deposition is a FACT-mediated deposition pathway. FACT, a H2A-H2B histone chaperone, is required for the H2A.Z deposition in budding yeast (Mahapatra et al., 2011). A recent paper shows that fission yeast FACT localizes at heterochromatin and is required for heterochromatic silencing through the

maintenance of H2A-H2B dynamics (Takahata et al., 2021). Thus, FACT might actively contribute to H2A.Z deposition at heterochromatic region. Another possibility is passive nucleosome assembly: histone chaperone independent nucleosome assembly has been reported (Newhart et al., 2013), and recent biochemical analysis has shown that H2A.Z-containing nucleosomes can be assembled more readily than canonical nucleosomes (Chen et al., 2019). These data raise the possibility that small amounts of H2A.Z are incorporated non-enzymatically into nucleosomes on replicated DNA at heterochromatic regions.

4-2 Functions of H2A.Z for heterochromatin assembly.

In this study, I showed a novel function of H2A.Z for H3K9me maintenance in the absence of RNAi. Since N-terminus of Pht1 is not involved in RNAi-independent heterochromatin assembly (Figure 27), the requirement of Pht1 in heterochromatin assembly is completely different from euchromatin roles of Pht1. Although *dcr1*Δ*pht1*Δ cells decreased H3K9me, H2A.Z is not required for TetR-Clr4 mediated artificial heterochromatin assembly, suggesting that H2A.Z does not directly enhance Clr4 self-propagation. Many factors including Rrp6 are required for RNAi-independent H3K9me assembly (Buscaino et al., 2013; Chalamcharla et al., 2015; Reyes-Turcu et al., 2011; Shipkovenska et al., 2020; Tucker et al., 2016), but the data in this study suggests that H2A.Z does not function in RNAi-independent H3K9me maintenance with Rrp6 (Figure 15).

Epe1 is an eraser of H3K9me *in vivo.* The balance between H3K9me deposition and Epe1-dependent demethylation determines the levels of H3K9me at both heterochromatin and euchromatin (Sorida et al., 2019). I have shown that Epe1 is responsible for the depletion of H3K9me in *dcr1*Δ*pht1*Δ cells at pericentromeres. This suggests that loss of H2A.Z in RNAi-deficient cells alters the competition between RNAi-independent H3K9 methylation and Epe1-mediated demethylation, resulting in the depletion of H3K9me at pericentromeres. By contrast, a decreased, but significant, level of H3K9me is retained at *mat* locus and subtelomeric heterochromatin in *dcr1*Δ*pht1*Δ cells, where Atf1/Pcr1-dependent and Taz1-dependent heterochromatin maintenance systems function, respectively. I believe that these H3K9me maintenance systems are sufficient to resist Epe1-mediated demethylation in the absence of H2A.Z. In addition, loss of Pht1 in *swi6*Δ cells did not alter H3K9me (Figure 12, 18). Since localization of Epe1 depends on Swi6

(Zofall and Grewal, 2006), Pht1 could not function in *swi6*Δ cells. This could also explain why loss of Pht1 in *dcr1*Δ cells did not increase *imr::ura4* expression (Figure 17), where H3K9me were abolished in *dcr1*Δ cells (Figure 21). Furthermore, as previously reported (Zofall et al., 2009), loss of Pht1 slightly increased H3K9me at all heterochromatic loci (Figure 12, 16, 18). Since loss of Epe1 considerably decreases siRNA (Trewick et al., 2007), Epe1-mediated transcription might be processed by RNAi pathway. In other words, Epe1 might be involved in the initiation of RNAi. Thus, I speculate that this slight increase of H3K9me is an effect of enhancement of RNAi.

Loss of H2A.Z does not affect Epe1 localization at heterochromatin and H2A.Z appears to directly inhibit Epe1-dependent demethylation. Epe1 has a JmjC histone demethylase catalytic domain, and many studies have shown that Epe1 induces H3K9me demethylation *in vivo* in a JmjC domain-dependent manner (Audergon et al., 2015; Ragunathan et al., 2015; Raiymbek et al., 2020; Sorida et al., 2019; Trewick et al., 2007). However, no enzymatic activity has been attributed to Epe1 *in vitro* (Raiymbek et al., 2020; Tsukada et al., 2006). Moreover, mutations in the JmjC domain affect the Epe1-Swi6 interaction (Raiymbek et al., 2020; Sorida et al., 2019), which makes it difficult to interpret experiments with JmjC domain mutants. Thus, it is still unclear whether Epe1 itself has enzymatic activity or not. It is possible that suppression occurs because H2A.Z-containing nucleosomes are poor substrates for Epe1-dependent demethylation. The crystal structures of homo- and heterotypic H2A.Z nucleosomes (H2A.Z/H2AZ and H2AZ/H2A, respectively) are quite similar but local differences are observed, and H2A.Z also enhances negative charge of the nucleosome surface, indicating the different protein interactions (Suto et al., 2000). H2A.Z enhances chromatin fiber compaction *in vitro* (Fan et al., 2004) and the deposition of H2A.Z on the genome has been shown to change chromatin accessibility (Berta et al., 2021). Indeed, H2A.Z is shown to promote H3K27 trimethylation and repress H3K4 trimethylation in plants (Dai et al., 2017). These properties may affect the recognition of substrates by the Epe1-mediated demethylation machinery.

I have also shown that H2A.Z suppresses Epe1-mediated transcription at subtelomeres (Figure 23). Furthermore, this suppression mechanism is independent of N-terminus (Figure 28), suggesting that it is different from the mechanism in euchromatin. It is possible that H2A.Z impedes Pol II progression initiated by Epe1

as H2A.Z acts as a barrier for transcription and inhibits Pol II transcription *in vivo* (Chen et al., 2019; Mylonas et al., 2021). Moreover, it is also possible that Epe1 removes H3K9me through histone turnover associated with transcription (Aygun et al., 2013), and that H2A.Z suppresses Epe1-mediated demethylation by suppressing Epe1-mediated transcription. Further investigation is required to understand the mechanism by which Epe1 demethylates *in vivo,* and how H2A.Z inhibits Epe1-mediated demethylation and transcriptional activation.

Heterochromatin is dynamically regulated during cell cycle. While RNAi is required for H3K9 di-methylation, self-propagation is responsible for the transition from H3K9me2 to H3K9me3 (Al-Sady et al., 2013; Jih et al., 2017), suggesting that both pathways are required for proper maintenance of heterochromatin. However, in principle, RNAi and Clr4 self-propagation could not occur at the same time because the requirement of RNA Pol II is completely different from each other; RNAi requires transcription, but self-propagation is inhibited by transcription (Audergon et al., 2015), suggesting that they work in different cell cycle stages. While Epe1 antagonizes Clr4 self-propagation (Audergon et al., 2015), Epe1 enhances siRNA formation which is required for RNAi pathway (Trewick et al., 2007). Thus, regulation of Epe1 is essential for controlling RNAi and Clr4 self-propagation. Therefore, H2A.Z may regulate the balance between RNAi pathway and Clr4 self-propagation through controlling the function of Epe1. Indeed, the deposition of H2A.Z is cell cycle dependent; for example, H2A.Z is accumulated at subtelomeric heterochromatin in M phase in mouse trophoblast stem cells (Nekrasov et al., 2012). It would be interesting to elucidate the requirement of H2A.Z and also Epe1 for the heterochromatin assembly during cell cycle.

4-3 H2A.Z compensates for the loss of H3K9me.

I have shown that loss of H2A.Z induces an increase in transcription from heterochromatic repeats when H3K9me is depleted by the loss of Clr4. Interestingly, this repression is not observed at marker genes inserted into the heterochromatin (Figure 16, 17), suggesting that this repression is heterochromatic repeat specific. I also found that the N-terminal region of H2A.Z is required for this repression. Since the N-terminal region of H2A.Z has been shown to be involved in the regulation of euchromatic genes in fission yeast, this mechanism of H2A.Z-dependent transcriptional repression in *clr4*Δ cells may partly overlap with that of euchromatic

gene regulation. Interestingly, both KQ and KR mutants increased ncRNAs transcribed from pericentromeric repeats in *clr4Δ* cells, and expression patterns of euchromatic genes in KQ and KR mutants are very similar (Kim et al., 2009), supporting the idea that H2A.Z functions at heterochromatic repeats in a similar way to at euchromatin genes. H2A.Z has various post translational modifications (Giaimo et al., 2019). In addition to the acetylation, N-terminus lysine is methylated, which has a repressive role (Binda et al., 2013), while acetylation is an active mark (Millar et al., 2006; Valdés-Mora et al., 2012). Therefore, I speculate that the repressive role of Pht1 in *clr4*Δ cells might be mediated by methylation as both KQ and KR mutants disrupts the effects of methylation. However, at this stage, detailed effects of N-terminus of Pht1 in heterochromatin and euchromatin are still unclear.

In mammals, loss of H3K9 or DNA methylation induces PRC recruitment and leads to the accumulation of methylated H3K27 to maintain gene silencing at the pericentromere (Puschendorf et al., 2008; Saksouk et al., 2014). This indicates that cells potentially have compensatory mechanisms. H2A.Z-dependent transcriptional repression at pericentromeric repeats might represent this compensatory mechanism in fission yeast, which does not have H3K27me and PRC. Constitutive heterochromatin often forms on repeated sequences. Repeated sequences facilitate homologous recombination, which would cause genome instability. Active transcription in the repeated sequences could further increase the probability that recombination occurs; indeed, a recent study in fission yeast has shown that transcription at pericentromeric repeats induces homologous recombination, resulting in gross chromosomal rearrangements in the absence of heterochromatin (Okita et al., 2019). Moreover, it has been reported that H2A.Z inhibits homologous recombination in human cells (Alatwi and Downs, 2015). Thus, deposition of H2A.Z and H2A.Z-dependent repression might contribute to genome stability by suppressing chromosomal rearrangements associated with compromised heterochromatin.

H2A.Z is essential for development in ES cells and *Xenopus laevis* (Faast et al., 2001; Ridgway et al., 2004); however, details are scarce. H2A.Z localizes at pericentromeres during ES cell differentiation (Rangasamy et al., 2003), suggesting that this essential role of H2A.Z in development might involve heterochromatic silencing. The findings in this study may have important implications for the understanding of the developmental role played by H2A.Z in other organisms.

5. References

Al-Sady, B., Madhani, Hiten D., and Narlikar, Geeta J. (2013). Division of Labor between the Chromodomains of HP1 and Suv39 Methylase Enables Coordination of Heterochromatin Spread. Molecular Cell *51*, 80-91.

Alatwi, H.E., and Downs, J.A. (2015). Removal of H2A.Z by INO80 promotes homologous recombination. EMBO reports *16*, 986-994.

Allshire, R.C., and Madhani, H.D. (2018). Ten principles of heterochromatin formation and function. Nat Rev Mol Cell Biol *19*, 229-244.

Altaf, M., Auger, A., Monnet-Saksouk, J., Brodeur, J., Piquet, S., Cramet, M., Bouchard, N., Lacoste, N., Utley, R.T., Gaudreau, L.*, et al.* (2010). NuA4-dependent Acetylation of Nucleosomal Histones H4 and H2A Directly Stimulates Incorporation of H2A.Z by the SWR1 Complex*. Journal of Biological Chemistry *285*, 15966-15977.

Anver, S., Roguev, A., Zofall, M., Krogan, N.J., Grewal, S.I.S., and Harmer, S.L. (2014). Yeast X-chromosome-associated protein 5 (Xap5) functions with H2A.Z to suppress aberrant transcripts. EMBO reports *15*, 894-902.

Audergon, P.N., Catania, S., Kagansky, A., Tong, P., Shukla, M., Pidoux, A.L., and Allshire, R.C. (2015). Restricted epigenetic inheritance of H3K9 methylation. Science *348*, 132-135.

Aygun, O., Mehta, S., and Grewal, S.I. (2013). HDAC-mediated suppression of histone turnover promotes epigenetic stability of heterochromatin. Nat Struct Mol Biol *20*, 547-554.

Ayoub, N., Noma, K., Isaac, S., Kahan, T., Grewal, S.I., and Cohen, A. (2003). A novel jmjC domain protein modulates heterochromatization in fission yeast. Mol Cell Biol *23*, 4356-4370.

Bayne, E.H., White, S.A., Kagansky, A., Bijos, D.A., Sanchez-Pulido, L., Hoe, K.L., Kim, D.U., Park, H.O., Ponting, C.P., Rappsilber, J.*, et al.* (2010). Stc1: a critical link between RNAi and chromatin modification required for heterochromatin integrity. Cell *140*, 666-677.

Berta, D.G., Kuisma, H., Välimäki, N., Räisänen, M., Jäntti, M., Pasanen, A., Karhu, A., Kaukomaa, J., Taira, A., Cajuso, T.*, et al.* (2021). Deficient H2A.Z deposition is associated with genesis of uterine leiomyoma. Nature *596*, 398-403.

Binda, O., Sevilla, A., LeRoy, G., Lemischka, I.R., Garcia, B.A., and Richard, S. (2013). SETD6 monomethylates H2AZ on lysine 7 and is required for the maintenance of embryonic stem cell self-renewal. Epigenetics *8*, 177-183.

Bönisch, C., and Hake, S.B. (2012). Histone H2A variants in nucleosomes and chromatin: more or less stable? Nucleic Acids Res *40*, 10719-10741.

Boyarchuk, E., Filipescu, D., Vassias, I., Cantaloube, S., and Almouzni, G. (2014). The histone variant composition of centromeres is controlled by the pericentric heterochromatin state during the cell cycle. Journal of Cell Science *127*, 3347-3359.

Buchanan, L., Durand-Dubief, M., Roguev, A., Sakalar, C., Wilhelm, B., Strålfors, A., Shevchenko, A., Aasland, R., Shevchenko, A., Ekwall, K.*, et al.* (2009). The Schizosaccharomyces pombe JmjC-Protein, Msc1, Prevents H2A.Z Localization in Centromeric and Subtelomeric Chromatin Domains. PLOS Genetics *5*, e1000726.

Buscaino, A., Lejeune, E., Audergon, P., Hamilton, G., Pidoux, A., and Allshire, R.C. (2013). Distinct roles for Sir2 and RNAi in centromeric heterochromatin nucleation, spreading and maintenance. EMBO J *32*, 1250-1264.

Chalamcharla, V.R., Folco, H.D., Dhakshnamoorthy, J., and Grewal, S.I. (2015). Conserved factor Dhp1/Rat1/Xrn2 triggers premature transcription termination and nucleates heterochromatin to promote gene silencing. Proc Natl Acad Sci U S A *112*, 15548-15555.

Chen, Z., Gabizon, R., Brown, A.I., Lee, A., Song, A., Díaz-Celis, C., Kaplan, C.D., Koslover, E.F., Yao, T., and Bustamante, C. (2019). High-resolution and high-accuracy topographic and transcriptional maps of the nucleosome barrier. eLife *8*, e48281.

Clayton, A.L., Hazzalin, C.A., and Mahadevan, L.C. (2006). Enhanced Histone Acetylation and Transcription: A Dynamic Perspective. Molecular Cell *23*, 289-296.

Creyghton, M.P., Markoulaki, S., Levine, S.S., Hanna, J., Lodato, M.A., Sha, K., Young, R.A., Jaenisch, R., and Boyer, L.A. (2008). H2AZ Is Enriched at Polycomb Complex Target Genes in ES Cells and Is Necessary for Lineage Commitment. Cell *135*, 649-661.

Daal, A.v., and Elgin, S.C. (1992). A histone variant, H2AvD, is essential in Drosophila melanogaster. Molecular Biology of the Cell *3*, 593-602.

Dai, X., Bai, Y., Zhao, L., Dou, X., Liu, Y., Wang, L., Li, Y., Li, W., Hui, Y., Huang, X.*, et al.* (2017). H2A.Z Represses Gene Expression by Modulating Promoter Nucleosome Structure and Enhancer Histone Modifications in Arabidopsis. Molecular Plant *10*, 1274-1292.

De Rop, V., Padeganeh, A., and Maddox, P.S. (2012). CENP-A: the key player behind centromere identity, propagation, and kinetochore assembly. Chromosoma *121*, 527-538.

Faast, R., Thonglairoam, V., Schulz, T.C., Beall, J., Wells, J.R., Taylor, H., Matthaei, K., Rathjen, P.D., Tremethick, D.J., and Lyons, I. (2001). Histone variant H2A.Z is required for early mammalian development. Curr Biol *11*, 1183-1187.

Fan, J.Y., Rangasamy, D., Luger, K., and Tremethick, D.J. (2004). H2A.Z Alters the Nucleosome Surface to Promote HP1α-Mediated Chromatin Fiber Folding. Molecular Cell *16*, 655-661.

Fischer, T., Cui, B., Dhakshnamoorthy, J., Zhou, M., Rubin, C., Zofall, M., Veenstra, T.D., and Grewal, S.I. (2009). Diverse roles of HP1 proteins in heterochromatin assembly and functions in fission yeast. Proc Natl Acad Sci U S A *106*, 8998-9003.

Gerace, E.L., Halic, M., and Moazed, D. (2010). The methyltransferase activity of Clr4Suv39h triggers RNAi independently of histone H3K9 methylation. Molecular cell *39*, 360-372.

Giaimo, B.D., Ferrante, F., Herchenröther, A., Hake, S.B., and Borggrefe, T. (2019). The histone variant H2A.Z in gene regulation. Epigenetics Chromatin *12*, 37.

Grewal, S.I., and Jia, S. (2007). Heterochromatin revisited. Nat Rev Genet *8*, 35-46.

Guillemette, B., Bataille, A.R., Gévry, N., Adam, M., Blanchette, M., Robert, F., and Gaudreau, L. (2005). Variant Histone H2A.Z Is Globally Localized to the Promoters of Inactive Yeast Genes and Regulates Nucleosome Positioning. PLOS Biology *3*, e384.

Hall, I.M., Shankaranarayana, G.D., Noma, K., Ayoub, N., Cohen, A., and Grewal, S.I. (2002). Establishment and maintenance of a heterochromatin domain. Science *297*, 2232-2237.

Hardy, S., Jacques, P.-É., Gévry, N., Forest, A., Fortin, M.-È., Laflamme, L., Gaudreau, L., and Robert, F. (2009). The Euchromatic and Heterochromatic Landscapes Are Shaped by Antagonizing Effects of Transcription on H2A.Z Deposition. PLOS Genetics *5*, e1000687.

Hong, J., Feng, H., Wang, F., Ranjan, A., Chen, J., Jiang, J., Ghirlando, R., Xiao, T.S., Wu, C., and Bai, Y. (2014). The Catalytic Subunit of the SWR1 Remodeler Is a Histone Chaperone for the H2A.Z-H2B Dimer. Molecular Cell *53*, 498-505.

Horikoshi, N., Arimura, Y., Taguchi, H., and Kurumizaka, H. (2016). Crystal structures of heterotypic nucleosomes containing histones H2A.Z and H2A. Open Biology *6*, 160127.

Hou, H., Wang, Y., Kallgren, S.P., Thompson, J., Yates, J.R., 3rd, and Jia, S. (2010). Histone variant H2A.Z regulates centromere silencing and chromosome segregation in fission yeast. J Biol Chem *285*, 1909-1918.

Iouzalen, N., Moreau, J., and Méchali, M. (1996). H2A.Zl, a New Variant Histone Expressed during Xenopus Early Development Exhibits Several Distinct Features from the Core Histone H2A. Nucleic Acids Research *24*, 3947-3952.

Jia, S., Noma, K., and Grewal, S.I. (2004). RNAi-independent heterochromatin nucleation by the stress-activated ATF/CREB family proteins. Science *304*, 1971-1976.

Jih, G., Iglesias, N., Currie, M.A., Bhanu, N.V., Paulo, J.A., Gygi, S.P., Garcia, B.A., and Moazed, D. (2017). Unique roles for histone H3K9me states in RNAi and heritable silencing of transcription. Nature *547*, 463-467.

Kanoh, J., Sadaie, M., Urano, T., and Ishikawa, F. (2005). Telomere Binding Protein Taz1 Establishes Swi6 Heterochromatin Independently of RNAi at Telomeres. Current Biology *15*, 1808-1819.

Kato, H., Goto, D.B., Martienssen, R.A., Urano, T., Furukawa, K., and Murakami, Y. (2005). RNA Polymerase II Is Required for RNAi-Dependent Heterochromatin Assembly. Science *309*, 467-469.

Kim, H.-S., Vanoosthuyse, V., Fillingham, J., Roguev, A., Watt, S., Kislinger, T., Treyer, A., Carpenter, L.R., Bennett, C.S., Emili, A.*, et al.* (2009). An acetylated form of histone H2A.Z regulates chromosome architecture in Schizosaccharomyces pombe. Nature structural & molecular biology *16*, 1286-1293.

Ladurner, A.G., Inouye, C., Jain, R., and Tjian, R. (2003). Bromodomains Mediate an Acetyl-Histone Encoded Antisilencing Function at Heterochromatin Boundaries. Molecular Cell *11*, 365-376.

Larson, A.G., Elnatan, D., Keenen, M.M., Trnka, M.J., Johnston, J.B., Burlingame, A.L., Agard, D.A., Redding, S., and Narlikar, G.J. (2017). Liquid droplet formation by HP1α suggests a role for phase separation in heterochromatin. Nature *547*, 236-240.

Liu, X., Li, B., and GorovskyMa (1996). Essential and nonessential histone H2A variants in Tetrahymena thermophila. Molecular and cellular biology *16*, 4305-4311.

Long, H., Zhang, L., Lv, M., Wen, Z., Zhang, W., Chen, X., Zhang, P., Li, T., Chang, L., Jin, C.*, et al.* (2020). H2A.Z facilitates licensing and activation of early replication origins. Nature *577*, 576-581.

Mahapatra, S., Dewari, P.S., Bhardwaj, A., and Bhargava, P. (2011). Yeast H2A.Z, FACT complex and RSC regulate transcription of tRNA gene through differential dynamics of flanking nucleosomes. Nucleic Acids Research *39*, 4023-4034.

Martire, S., and Banaszynski, L.A. (2020). The roles of histone variants in fine-tuning chromatin organization and function. Nature Reviews Molecular Cell Biology *21*, 522-541.

Millar, C.B., Xu, F., Zhang, K., and Grunstein, M. (2006). Acetylation of H2AZ Lys 14 is associated with genome-wide gene activity in yeast. Genes Dev *20*, 711-722.

Mizuguchi, G., Shen, X., Landry, J., Wu, W.H., Sen, S., and Wu, C. (2004). ATP-driven exchange of histone H2AZ variant catalyzed by SWR1 chromatin remodeling complex. Science *303*, 343-348.

Motamedi, M.R., Hong, E.J., Li, X., Gerber, S., Denison, C., Gygi, S., and Moazed, D. (2008). HP1 proteins form distinct complexes and mediate heterochromatic gene silencing by nonoverlapping mechanisms. Mol Cell *32*, 778-790.

Motamedi, M.R., Verdel, A., Colmenares, S.U., Gerber, S.A., Gygi, S.P., and Moazed, D. (2004). Two RNAi complexes, RITS and RDRC, physically interact and localize to noncoding centromeric RNAs. Cell *119*, 789-802.

Mylonas, C., Lee, C., Auld, A.L., Cisse, I.I., and Boyer, L.A. (2021). A dual role for H2A.Z.1 in modulating the dynamics of RNA polymerase II initiation and elongation. Nature Structural & Molecular Biology.

Nakayama, J., Rice, J.C., Strahl, B.D., Allis, C.D., and Grewal, S.I. (2001). Role of histone H3 lysine 9 methylation in epigenetic control of heterochromatin assembly. Science *292*, 110-113.

Nekrasov, M., Amrichova, J., Parker, B.J., Soboleva, T.A., Jack, C., Williams, R., Huttley, G.A., and Tremethick, D.J. (2012). Histone H2A.Z inheritance during the cell cycle and its impact on promoter organization and dynamics. Nat Struct Mol Biol *19*, 1076-1083.

Newhart, A., Rafalska-Metcalf, I.U., Yang, T., Joo, L.M., Powers, S.L., Kossenkov, A.V., Lopez-Jones, M., Singer, R.H., Showe, L.C., Skordalakes, E.*, et al.* (2013). Single cell analysis of RNA-mediated histone H3.3 recruitment to a cytomegalovirus promoter-regulated transcription site. J Biol Chem *288*, 19882-19899.

Noma, K., Allis, C.D., and Grewal, S.I. (2001). Transitions in distinct histone H3 methylation patterns at the heterochromatin domain boundaries. Science *293*, 1150-1155.

Okita, A.K., Zafar, F., Su, J., Weerasekara, D., Kajitani, T., Takahashi, T.S., Kimura, H., Murakami, Y., Masukata, H., and Nakagawa, T. (2019). Heterochromatin suppresses gross chromosomal rearrangements at centromeres by repressing Tfs1/TFIIS-dependent transcription. Communications Biology *2*, 17.

Olson, N.M., Kroc, S., Johnson, J.A., Zahid, H., Ycas, P.D., Chan, A., Kimbrough, J.R., Kalra, P., Schönbrunn, E., and Pomerantz, W.C.K. (2020). NMR Analyses of Acetylated H2A.Z Isoforms Identify Differential Binding Interactions with the Bromodomain of the NURF Nucleosome Remodeling Complex. Biochemistry *59*, 1871-1880.

Pokholok, D.K., Harbison, C.T., Levine, S., Cole, M., Hannett, N.M., Lee, T.I., Bell, G.W., Walker, K., Rolfe, P.A., Herbolsheimer, E.*, et al.* (2005). Genome-wide map of nucleosome acetylation and methylation in yeast. Cell *122*, 517-527.

Provost, P., Silverstein, R.A., Dishart, D., Walfridsson, J., Djupedal, I., Kniola, B., Wright, A., Samuelsson, B., Rådmark, O., and Ekwall, K. (2002). Dicer is required for chromosome segregation and gene silencing in fission yeast cells. Proceedings of the National Academy of Sciences *99*, 16648-16653.

Puschendorf, M., Terranova, R., Boutsma, E., Mao, X., Isono, K.-i., Brykczynska, U., Kolb, C., Otte, A.P., Koseki, H., Orkin, S.H.*, et al.* (2008). PRC1 and Suv39h specify parental asymmetry at constitutive heterochromatin in early mouse embryos. Nature Genetics *40*, 411-420.

Ragunathan, K., Jih, G., and Moazed, D. (2015). Epigenetic inheritance uncoupled from sequence-specific recruitment. Science *348*, 1258699.

Raisner, R.M., Hartley, P.D., Meneghini, M.D., Bao, M.Z., Liu, C.L., Schreiber, S.L., Rando, O.J., and Madhani, H.D. (2005). Histone variant H2A.Z marks the 5' ends of both active and inactive genes in euchromatin. Cell *123*, 233-248.

Raiymbek, G., An, S., Khurana, N., Gopinath, S., Larkin, A., Biswas, S., Trievel, R.C., Cho, U.-s., and Ragunathan, K. (2020). An H3K9 methylation-dependent protein interaction regulates the non-enzymatic functions of a putative histone demethylase. eLife *9*, e53155.

Rangasamy, D., Berven, L., Ridgway, P., and Tremethick, D.J. (2003). Pericentric heterochromatin becomes enriched with H2A.Z during early mammalian development. Embo j *22*, 1599-1607.

Ranjan, A., Mizuguchi, G., FitzGerald, Peter C., Wei, D., Wang, F., Huang, Y., Luk, E., Woodcock, Christopher L., and Wu, C. (2013). Nucleosome-free Region Dominates Histone Acetylation in Targeting SWR1 to Promoters for H2A.Z Replacement. Cell *154*, 1232-1245.

Ranjan, A., Nguyen, V.Q., Liu, S., Wisniewski, J., Kim, J.M., Tang, X., Mizuguchi, G., Elalaoui, E., Nickels, T.J., Jou, V.*, et al.* (2020). Live-cell single particle imaging reveals the role of RNA polymerase II in histone H2A.Z eviction. eLife *9*, e55667.

Reyes-Turcu, F.E., Zhang, K., Zofall, M., Chen, E., and Grewal, S.I. (2011). Defects in RNA quality control factors reveal RNAi-independent nucleation of heterochromatin. Nat Struct Mol Biol *18*, 1132-1138.

Ridgway, P., Brown, K.D., Rangasamy, D., Svensson, U., and Tremethick, D.J. (2004). Unique residues on the H2A.Z containing nucleosome surface are important for Xenopus laevis development. J Biol Chem *279*, 43815-43820.

Rose, N.R., and Klose, R.J. (2014). Understanding the relationship between DNA methylation and histone lysine methylation. Biochimica et Biophysica Acta (BBA) - Gene Regulatory Mechanisms *1839*, 1362-1372.

Sabatinos, S.A., and Forsburg, S.L. (2010). Chapter 32 - Molecular Genetics of Schizosaccharomyces pombe. In Methods in Enzymology (Academic Press), pp. 759-795.

Sadaie, M., Iida, T., Urano, T., and Nakayama, J.-i. (2004). A chromodomain protein, Chp1, is required for the establishment of heterochromatin in fission yeast. The EMBO Journal *23*, 3825-3835.

Saksouk, N., Barth, T.K., Ziegler-Birling, C., Olova, N., Nowak, A., Rey, E., Mateos-Langerak, J., Urbach, S., Reik, W., Torres-Padilla, M.E.*, et al.* (2014). Redundant mechanisms to form silent chromatin at pericentromeric regions rely on BEND3 and DNA methylation. Mol Cell *56*, 580-594.

Shipkovenska, G., Durango, A., Kalocsay, M., Gygi, S.P., and Moazed, D. (2020). A conserved RNA degradation complex required for spreading and epigenetic inheritance of heterochromatin. Elife *9*.

Sorida, M., Hirauchi, T., Ishizaki, H., Kaito, W., Shimada, A., Mori, C., Chikashige, Y., Hiraoka, Y., Suzuki, Y., Ohkawa, Y*., et al.* (2019). Regulation of ectopic heterochromatin-mediated epigenetic diversification by the JmjC family protein Epe1. PLOS Genetics *15*, e1008129.

Suto, R.K., Clarkson, M.J., Tremethick, D.J., and Luger, K. (2000). Crystal structure of a nucleosome core particle containing the variant histone H2A.Z. Nat Struct Biol *7*, 1121-1124.

Takahata, S., Chida, S., Ohnuma, A., Ando, M., Asanuma, T., and Murakami, Y. (2021). Two secured FACT recruitment mechanisms are essential for heterochromatin maintenance. Cell Reports *36*.

Talbert, P.B., and Henikoff, S. (2014). Environmental responses mediated by histone variants. Trends in Cell Biology *24*, 642-650.

Touat-Todeschini, L., Shichino, Y., Dangin, M., Thierry-Mieg, N., Gilquin, B., Hiriart, E., Sachidanandam, R., Lambert, E., Brettschneider, J., Reuter, M*., et al.* (2017). Selective termination of lncRNA transcription promotes heterochromatin silencing and cell differentiation. The EMBO Journal *36*, 2626-2641.

Tramantano, M., Sun, L., Au, C., Labuz, D., Liu, Z., Chou, M., Shen, C., and Luk, E. (2016). Constitutive turnover of histone H2A.Z at yeast promoters requires the preinitiation complex. eLife *5*, e14243.

Trewick, S.C., Minc, E., Antonelli, R., Urano, T., and Allshire, R.C. (2007). The JmjC domain protein Epe1 prevents unregulated assembly and disassembly of heterochromatin. EMBO J *26*, 4670-4682.

Tsukada, Y., Fang, J., Erdjument-Bromage, H., Warren, M.E., Borchers, C.H., Tempst, P., and Zhang, Y. (2006). Histone demethylation by a family of JmjC domain-containing proteins. Nature *439*, 811-816.

Tucker, J.F., Ohle, C., Schermann, G., Bendrin, K., Zhang, W., Fischer, T., and Zhang, K. (2016). A Novel Epigenetic Silencing Pathway Involving the Highly Conserved 5'-3' Exoribonuclease Dhp1/Rat1/Xrn2 in Schizosaccharomyces pombe. PLOS Genetics *12*, e1005873.

Valdés-Mora, F., Song, J.Z., Statham, A.L., Strbenac, D., Robinson, M.D., Nair, S.S., Patterson, K.I., Tremethick, D.J., Stirzaker, C., and Clark, S.J. (2012). Acetylation of H2A.Z is a key epigenetic modification associated with gene deregulation and epigenetic remodeling in cancer. Genome Res *22*, 307-321.

Verdel, A., Jia, S., Gerber, S., Sugiyama, T., Gygi, S., Grewal, S.I., and Moazed, D. (2004). RNAi-mediated targeting of heterochromatin by the RITS complex. Science *303*, 672-676.

Volpe, T.A., Kidner, C., Hall, I.M., Teng, G., Grewal, S.I., and Martienssen, R.A. (2002). Regulation of heterochromatic silencing and histone H3 lysine-9 methylation by RNAi. Science *297*, 1833-1837.

Wang, J., Cohen, A.L., Letian, A., Tadeo, X., Moresco, J.J., Liu, J., Yates, J.R., 3rd, Qiao, F., and Jia, S. (2016). The proper connection between shelterin components is required for telomeric heterochromatin assembly. Genes Dev *30*, 827-839.

Watson, A.T., Werler, P., and Carr, A.M. (2011). Regulation of gene expression at the fission yeast Schizosaccharomyces pombe urg1 locus. Gene *484*, 75-85.

Wiles, E.T., and Selker, E.U. (2017). H3K27 methylation: a promiscuous repressive chromatin mark. Current Opinion in Genetics & Development *43*, 31-37.

Yamada, T., Fischle, W., Sugiyama, T., Allis, C.D., and Grewal, S.I. (2005). The nucleation and maintenance of heterochromatin by a histone deacetylase in fission yeast. Mol Cell *20*, 173-185.

Yen, K., Vinayachandran, V., and Pugh, B.F. (2013). SWR-C and INO80 Chromatin Remodelers Recognize Nucleosome-free Regions Near +1 Nucleosomes. Cell *154*, 1246-1256.

Zeng, L., and Zhou, M.M. (2002). Bromodomain: an acetyl-lysine binding domain. FEBS Lett *513*, 124-128.

Zhang, H., Roberts, D.N., and Cairns, B.R. (2005). Genome-Wide Dynamics of Htz1, a Histone H2A Variant that Poises Repressed/Basal Promoters for Activation through Histone Loss. Cell *123*, 219-231.

Zilberman, D., Coleman-Derr, D., Ballinger, T., and Henikoff, S. (2008). Histone H2A.Z and DNA methylation are mutually antagonistic chromatin marks. Nature *456*, 125-129.

Zlatanova, J., and Thakar, A. (2008). H2A.Z: view from the top. Structure *16*, 166-179.

Zofall, M., Fischer, T., Zhang, K., Zhou, M., Cui, B., Veenstra, T.D., and Grewal, S.I. (2009). Histone H2A.Z cooperates with RNAi and heterochromatin factors to suppress antisense RNAs. Nature *461*, 419-422.

Zofall, M., and Grewal, S.I. (2006). Swi6/HP1 recruits a JmjC domain protein to facilitate transcription of heterochromatic repeats. Mol Cell *22*, 681-692.

Zofall, M., Smith, D.R., Mizuguchi, T., Dhakshnamoorthy, J., and Grewal, S.I.S. (2016). Taz1-Shelterin Promotes Facultative Heterochromatin Assembly at Chromosome-Internal Sites Containing Late Replication Origins. Mol Cell *62*, 862-874.

6. Acknowledgements

I would like to express my great appreciation to my supervisor Professor Yota Murakami for his encouragement, extensive discussions, and critical advice.

I would like to thank Professor Kazuyasu Sakaguchi, Professor Akinori Takaoka, and Professor Mutsumi Takagi for their helpful suggestions.

I am grateful to Specially Appointed Lecturer Shinya Takahata for his encouragement, technical support, and useful discussions.

I wish to thank all of the previous and current members of Laboratory of Bioorganic Chemistry, especially Mr. Takahiro Asanuma, Dr. Masato Sorida, Mr. Takahiro Hirauchi, Dr. Shota Suzuki and Dr. Eriko Oya for helpful discussions and technical supports.

I would like to express my gratitude to Professor Jun-ichi Nakayama and Professor Robin Allshire for providing strains, Professor Hiroshi Kimura for providing antibodies.

Finally, I would like to thank my parents for their financial support and constant encouragement.